

Faculty of Science and Technology

MASTER'S THESIS

Study program/Specialization:

Spring semester, 2022

Engineering Structures and Materials/ Civil Structures

Open access

Writer: **Enes Hacıhamud**

A handwritten signature in black ink, appearing to be 'Enes Hacıhamud'.

(Writer's signature)

Faculty supervisor:

Hirpa G. Lemu, UiS

Sudath C. Siriwardane, UiS

External advisor(s):

Kjetil Dahl, DNV

Ole Gabrielsen, DNV

Thesis title:

Non-Linear Buckling Analysis of Stiffened Panels

Credits (ECTS): **30**

Keywords:

**Buckling
Non-Linear
Stiffened Panels**

Pages: 57

Stavanger, June, 2022

Abstract

Nonlinear buckling capacity analysis has become a reliable practice in order to investigate the buckling capacities for cases that do not fall into the scope of the traditional standards. DNV has issued the recommended practice DNV-RP-C208 [3] as a guideline for nonlinear finite element buckling analysis.

The project aims to apply nonlinear finite element methods to evaluate the buckling capacity of a ship hull stiffened panel under uniaxial in-plane compression load and gravity load. Then, to calibrate and compare the results to conventional codes, this is done by determining the buckling capacity of the panel using "DNV-RP-C201 Buckling Strength of Plated Structures" to establish a capacity benchmark. Then, the finite element analysis program ABAQUS is used to build a stiffened panel model and introduce the material and geometrical nonlinearities using the method outlined in the recommended practice "DNV-RP-C208, Determination of structural capacity by nonlinear finite element analysis methods" to achieve the calibration to the benchmark buckling capacity.

The calibration is achieved by studying the effect of two different geometrical imperfection patterns with several different magnitudes. This is used to choose the model with imperfections pattern and magnitude that would provide the buckling capacities closer to the benchmark as a calibrated model. It is then used to study the effect of holes on the buckling capacity of the panel.

Acknowledgement

This research project is submitted to fulfil the requirement to complete a Master of Science in Engineering Structures and Material, at the Faculty of Science and Technology, University of Stavanger, Norway. The thesis topic is proposed by DNV and is carried out in the company's premises, during spring academic year 2022.

My gratitude goes to Det Norske Veritas (DNV), Stavanger, Norway for providing me with office space, computer system, full support and access to standards and ABAQUS Finite element software and other software to facilitate successful execution of this research.

I would especially like to thank my day-to-day supervisor, senior engineer Kjetil Dahl from DNV, Stavanger. For his guidance, advice, time for sharing knowledge and continuous support at every step of this thesis. I would like to offer my sincere gratitude Ole Gabrielsen from DNV for the support and guidance through this research. I would like to emphasize that I am extremely grateful to Kjetil and Ole and that it was a privilege to work with them.

I would like to thank my supervisors Professor Hirpa Gelgele Lemu and Professor Sudath C. Siriwardane from the University of Stavanger, for their close guidance and management of the project. Also, I would like to appreciate engineers Andreas Aaslid and Anders Lysø Kleven from DNV for their assistance regarding the finite element modeling using ABAQUS.

Finally, I am also grateful for my mother Dr. Azza Obysi and my father Dr. Bashar Hamoud, for their support during my studies and through this master thesis.

Enes Hacıhamud

Stavanger , Norway

15.06.2022

Contents

List of Figures.....	V
List of Tables.....	VII
List of Abbreviations	VIII
Symbols.....	IX
Chapter- 1 Introduction.....	1
1.1 Background and Motivation.....	1
1.2 Research objective.....	2
1.3 Research gap and challenges	2
1.4 Methodological approach	3
1.5 Thesis structure.....	4
Chapter- 2 Literature Study.....	5
2.1 Literature review.....	5
2.2 Buckling capacity according to DNV-RP- C201.....	8
2.2.1 Design by LRFD method	8
2.2.2 Ultimate limit state (ULS).....	9
2.2.3 Stiffener type	10
2.2.4 Buckling length	10
2.2.5 Bending moment factors K_m	11
2.2.6 Geometry	11
2.2.7 Buckling check procedure according to DNV-RP-C201 :.....	12
2.3 Non-linear buckling capacity according to DNV-RP-C208.....	14
Chapter- 3 Establishing benchmark buckling capacity according to DNV-RP-C201	16
3.1 Safety format.....	16
3.2 Stiffener type and geometry	16
3.3 Buckling length and bending moment factors K_m	17
3.4 Geometry and material properties.....	17
3.5 Applied stresses	18
3.6 Buckling check results according to DNV-RP-C201.....	19
Chapter- 4 Finite Element Model Description of Ship Hull Stiffened Panel.....	21
4.1 Geometrical properties	21
4.2 Non-linear Material properties	23
4.3 Applied force	24
4.4 Boundary conditions.....	24
Chapter- 5 Non-linear Finite Element Analysis of Stiffened Ship Hull Panel	26

5.1	Introduction and Assumptions.....	26
5.2	Element type	26
5.3	Mesh size	26
5.4	Introducing the Geometrical Imperfection to the model	29
5.5	Eigenmode analysis.....	31
5.6	Results.....	39
Chapter- 6	Discussion and Compression of the Results	49
6.1	Discussion of results of non-linear analysis	49
6.2	Discussion of calibration case results	51
6.3	Effect of holes on buckling capacity of the calibrated model.....	54
Chapter- 7	Conclusion and Recommendation for Further Work.....	56
7.1	Summary.....	56
7.2	Concluding remarks	56
7.3	Recommendation for further work	57
References	58
Appendix	59

List of Figures

Figure 1: Illustration of stiffened panels (DNV-RP-C208)	1
Figure 2- Stiffened panel	5
Figure 3-Illustration of the limit state safety format [3]	8
Figure 4-Structural design considerations based on the ultimate limit state[6]	10
Figure 5- Continuous stiffener [12]	10
Figure 6-Sniped stiffener[12].....	10
Figure 7- Idealized stiffined panel [12]	11
Figure 9-Geometrical properties of stiffeners	16
Figure 10- Applied loads in buckling capacity according to DNV-RP-C201	18
Figure 11-Plate-Stiffener buckling ckeck-1.....	20
Figure 12-Plate stiffener buckling check-	20
Figure 13- Real ship hull stiffened panel model.....	21
Figure 14-Non-linear material properties- stress-strain relation	23
Figure 15-Non-linear material stress-strain relation	23
Figure 16- Real Ship hull stiffened panel boundary conditions	24
Figure 16 FE-model boundary conditions	25
Figure 18-Mesh sensitivity study	27
Figure 18- Mesh-3 used in the FE non-linear model	28
Figure 19-Examples of buckling curves showing sensitivity for imperfections etc. for different forms [3]	29
Figure 23	29
Figure 25 DNV-RP-C208 recommended Local Imperfection pattern (left),global Imperfection pattern (right).....	29
Figure 29- Global imperfection pattern.....	32
Figure 32-Local imperfection pattern 1	34
Figure 35-Local imperfection pattern-2	35
Figure 36- Global imperfection pattern nodal displacement distribution	36
Figure 37-Local imperfection pattern 1 nodal displacement distribution	37
Figure 38--Local imperfection pattern 2 nodal displacement distribution	38
Figure 39-Combined imperfection pattern-Case 1	39
Figure 40- Combined imperfection pattern-Case 2	40
Figure 41- Case 1/SF1 non-linear buckling capacity	41
Figure 42-Case 1/SF2 non-linear buckling capacity	42
Figure 43-Case 1/SF3 non-linear buckling capacity	43
Figure 44-Case 1/SF4 non-linear buckling capacity	44
Figure 45-Case 1/SF5 non-linear buckling capacity	45
Figure 46-Case 2/SF1 non-linear buckling capacity	46
Figure 47--Case 2/SF2 non-linear buckling capacity	47
Figure 48--Case 2/SF3 non-linear buckling capacity	48
Figure 49- Comparison of the combined patterns cases, nonlinear buckling analysis results	49
Figure 50- Calibrated case imperfection magnitude and distribution	51
Figure 51- Von-mises stress distribution (MPa)	52
Figure 52- Panel stress concentration	53
Figure 53-Panel strain concentration	53

Figure 54- Calibrated model- Hole 1..... 54
Figure 55- Calibrated model Hole 2 54
Figure 56- Effect of holes on calibrated model buckling capacity 55
Figure 57 Plate-Stiffener buckling check using 59
Figure 58 Plate-stiffener yield and section checks 60
Figure 59- Parameters used in Stiffener plate checks 61
Figure 60 Girder Buckling check 62
Figure 61- Girder yield check..... 62
Figure 62 Girder yield and buckling check..... 63

List of Tables

Table 1- Methodological approach	3
Table 2- Bending moment and shear force factors K_m	11
Table 3- Stiffener geometrical properties	16
Table 4- Panel geometry	17
Table 5- Geometrical properties of FE model	22
Table 6- Non-linear material properties	23
Table 7- FE model boundary conditions	24
Table 8- Mesh sensitivity- element size assessment	27
Table 9- DNVRP-C208 imperfection amplitude recommendation	30
Table 10- Global Imperfection pattern average displacement	37
Table 11- local imperfection pattern 1 average displacements	37
Table 12- Local imperfection pattern 2 average displacement	38
Table 13- Applied scale factors	38
Table 14- Case1/SF1 Capacity deviation percentage	41
Table 15- Case1/SF2 Capacity deviation percentage	42
Table 16- Case1/SF3 Capacity deviation percentage	43
Table 17- Case1/SF4 Capacity deviation percentage	44
Table 18- Case1/SF5 Capacity deviation percentage	45
Table 19- Case2/SF1 Capacity deviation percentage	46
Table 20- Case2/SF2 Capacity deviation percentage	47
Table 21- Case2/SF3 Capacity deviation percentage	48
Table 22- Result summary	49
Table 23- Effects of holes on buckling capacity of the calibrated model	55

List of Abbreviations

ABAQUS ANALYSIS PROGRAM

CS Cross-Section

DNV Det Norske Veritas

FEA Finite Element Analysis

FE Finite Element

OS Offshore Standard

RP Recommended Practice

STIPLA Buckling analysis program based in DNV standards

SF Scale Factor

Symbols

A	cross sectional area
A_e	effective area
A_f	cross sectional area of flange
A_G	cross-sectional area of girder
A_s	cross sectional area of stiffener
A_w	cross sectional area of web
E	<i>Young's</i> modulus
E_{p1}	stress-strain curve parameter
E_{p2}	stress-strain curve parameter
F_y	yield stress/yield strength
F_L	local pattern scale factor
F_G	Global pattern scale factor
h_w	height of stiffener web
K	Ramberg-Osgood parameter
K_m	Bending moment factors
L	Stiffener span
L_g	length of girder
L_t	lateral torsional buckling length
$M_{1,Sd}$	design bending moment at point 1
$M_{2,Sd}$	design bending moment at point 2
$M_{s2,Rd}$	design bending moment resistance on stiffener side at point 2
$M_{p,Rd}$	plate side design bending moment resistance
$M_{st,Rd}$	design bending moment resistance on stiffener side in tension
N_E	Euler buckling strength
N_{Sd}	design axial force
N_{Rd}	buckling axial resistance
$N_{kp,Rd}$	design plate induced axial buckling resistance
$N_{ks,Rd}$	stiffener induced design axial buckling resistance
N	number of cycles to failure

R_d	design resistance
R_k	characteristic resistance
S	stiffener spacing
S_d	design action effect
t	plate thickness
t_f	flange thickness
U_L	the nodal displacement introduced by the local pattern
U_g	the nodal displacement introduced by the global pattern
$U_{av,max}$	Maximum mid-span nodal average displacement
$U_{av,min}$	Minimum mid-span nodal average displacement
u	the design shear stress to the design resistance shear stress squared ratio
z^*	distance from the neutral axis of the effective section to the point of the axial force
ε	strain
$\varepsilon_{p,y1}$	stress-strain curve parameter
σ_{prop}	stress-strain curve parameter
σ_{yield}	stress-strain curve parameter
σ_{yield2}	stress-strain curve parameter
σ_{ult}	stress-strain curve parameter

Chapter- 1 Introduction

1.1 Background and Motivation

Stiffened panels (Figure 1) are commonly used in many industries, especially offshore and maritime sectors. This is due to its high load and stiffness-to-weight ratio capability. Since buckling is one of the common failure modes of stiffened panels, it has been widely researched through the years using analytical methods, experimental tests, and non-linear elements (FE).

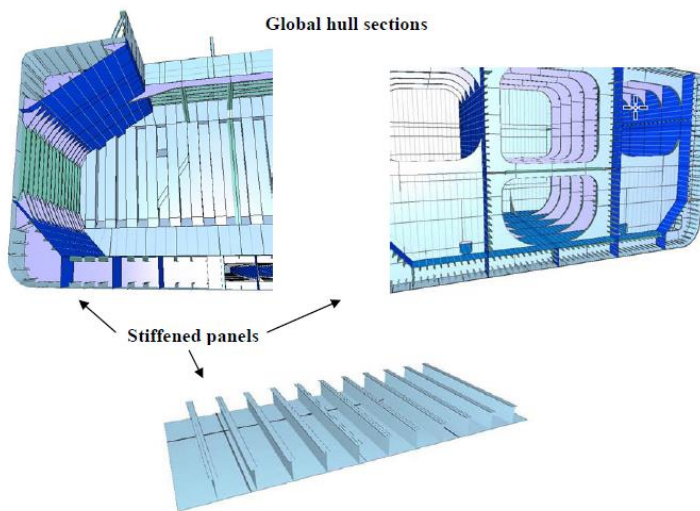


Figure 1: Illustration of stiffened panels (DNV-RP-C208)

Guidance for designing against buckling failure is available in several standards such as DNV-RP-C201[1] and NS-EN 1993-1-5 [2]. These standards predict failure capacities for plated structures.

In some cases that are not included in the scope of the standards above, non-linear finite element analyses can be used to determine the capacity. Guidance and recommended practices have been developed for these methods, such as the DNV recommended practice DNVGL-RP-C208 [3].

1.2 Research objective

The project aims to apply non-linear finite element methods to evaluate the buckling capacity of stiffened panels and calibrate and compare the results to conventional codes. This is done by determining the buckling capacity of the panel using “DNV-RP-C201[1] Buckling Strength of Plated Structures” to establish a capacity benchmark. Then, using the finite element analysis program ABAQUS to build a stiffened panel model and introduce the material and geometrical nonlinearities to achieve the calibration to the benchmark buckling capacities. The calibration is achieved by studying the effect of two different geometrical imperfection patterns with several different magnitudes to choose the model with imperfections pattern and magnitude that would provide the buckling capacities closer to the benchmark as a calibrated model. It is then used to study the effect of holes in the panel in the buckling capacity of the panel.

1.3 Research gap and challenges

The research gap is summarized as the lack of studies on achieving calibration of buckling capacity of large ship hull stiffened panel using the DNV-RP-C201[1] standard as a capacity benchmark and the recommended practice DNV-RP-C208[3] guidelines for non-linear FE buckling analysis.

The challenges with regard to the non-linear buckling capacity analysis are listed below,

- Introducing applicable rule required geometrical nonlinearity in the finite element model.
- Identifying issues with material nonlinearity and evaluating the consequences of large strains.
- Choosing a set of boundary conditions that represent the physical problem appropriately.
- Introducing a combined local and global imperfections into the finite element model.
- Achieving calibration of ABAQUS model to DNV-RP-C201[1] using the method outlined in DNV-RP-C208[3]. Then presenting the analysis results in a way that clearly induces confidence in this calibration.

1.4 Methodological approach

The methodology of the thesis is summarized in Table 1.

Table 1- Methodological approach

APPROACH	DESCRIPTION
Pre-study report	A report is prepared to explain the plan of the thesis project and set the goal and objectives
Literature study of buckling codes and nonlinearity	Familiarization with recommended practices “DNV-RP-C201[1] Buckling strength of plated structures” and “DNV-RP-C208 [3] determination of structural capacity by non-linear finite element analysis methods.”
Selecting geometries and loads	Selecting the stiffened panel type and geometrical properties of a commonly used stiffened panels in offshore and marine steel structures under compression loads.
Establishing calibration capacity benchmark	Buckling capacity of the selected geometry using the DNV-RP-C201[1] code.
Building finite element model	Using ABAQUS as a FEM structural analysis program.
Eigenvalue analysis	Performing eigenmode analysis to acquire imperfection patterns and magnitudes to be mapped into the model.
Choosing imperfection patterns	Evaluating the eigenmodes to choose the ones that are closest to the modes recommended by DNV-RP-C208 [3].
Calibrating non-linear model to DNV-RP-C201	Performing a study on the effects of the introduced geometrical imperfection magnitude on the buckling capacity in order to achieve calibration buckling capacity.
Calibration post-processing	Comparing the results, explaining, and discussing the findings concerning the applied nonlinearities and codes.
Evaluation of the effect of holes	Evaluating the effect of holes on the buckling capacity of calibrated non-linear FE model
Reporting	Reporting the work done.

1.5 Thesis structure

This report includes 7 chapters. The description of the content of each chapter is shown below:

Chapter 1 Introduction

This chapter includes the motivation and background. It also describes the research gap and the methodology used in the thesis.

Chapter 2 literature study

This chapter includes the literature review and describes the approaches used in finding buckling capacity according to DNV-RP-C201[1] standard. It also describes the approach used in determining the non-linear buckling capacity according to DNV-RP-C208 [3] recommended practice.

Chapter 3 Establishing benchmark buckling capacity according to DNV-RP-C201

The buckling capacity according to DNV-C201 is established in this chapter. It also explains the parameters used to assess the buckling capacity.

Chapter 4. Finite element Model description of ship hull stiffened panel

This chapter describes the ship hull panel properties used to model in FE program.

Chapter 5 Non-linear finite element analysis of stiffened ship hull panel

The non-linear buckling analysis and the calibration of the model to the buckling capacity benchmark are carried out in this chapter.

Chapter 6- Results and discussion

This chapter presents and compares the results found by the non-linear analyses. It explains the most compatible calibrated case. The chapter also evaluates the effect of holes on the buckling capacity of the calibrated model.

Chapter 7- Conclusion and Recommendation for Further Work

A summary of the work performed, the conclusion of the thesis, and suggestions for further work take place in this chapter.

Chapter- 2 Literature Study

2.1 Literature review

Stiffened panels -as shown in Figure 2- are an assembly of plates, stiffeners and girders. In order to increase the strength and capacity of the plate to carry in-plane and out-of-plane loads, the plate is attached to stiffeners [4]. Stiffened panels are used in different branches of engineering, especially in offshore or ship structures where they are constructed as an assembly of stiffened plates with almost equally spaced longitudinal stiffeners of the same size. Buckling and plastic collapse of the ship hulls govern the overall failure of ships. For this reason, it is essential to precisely analyze the ultimate strength of the stiffened panels in ship hull.

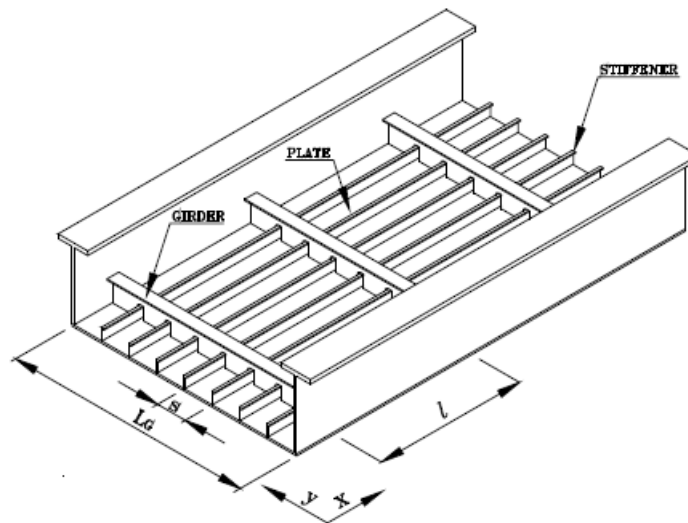


Figure 2- Stiffened panel

Buckling is caused by in-plane stresses exceeding the buckling stability of the structure, causing local yield and permanent deformation of the structure. The buckling capacity is a property of the plate, depending on many factors.[5]

Buckling can be classified into three states:

1. Elastic buckling: occurs only in the elastic regime of the stress-strain material graph.
2. Elasto-plastic buckling: occurs when a local region inside the plate experiences a plastic deformation.
3. Plastic buckling: happens after the plate has yielded over large regions.[6]

Many factors affect the buckling behaviors of panels, including geometric or material properties, loading characteristics, boundary conditions, initial geometrical imperfections, and material nonlinearity. If the panel is welded, the residual stresses also affect the buckling behavior. Under the same conditions and properties, panels with high slenderness show plastic buckling, while low slenderness panels show elastic buckling [3].

In the linear analysis, materials are assumed to be in the linear elastic region. The linear analysis assumes very small displacements during and after loading so that equilibrium and kinematic relations are applied to undeformed geometry. Also, contrary to non-linear analysis, superposition is applicable to the linear solution. The linear models provide acceptable approximations for many practical problems.

Linear elastic finite element analyses of the load effects are used for the design check of plated structures [1]. Moreover, the ultimate strength of offshore structures is analyzed by linear methods to determine the internal distribution of forces, moments. The resistances of the cross-sections are checked according to design resistances found in design standards. These design resistance formulas often require deformations well into the inelastic range in order to mobilize the standard defined resistances. However, no further checks are normally considered necessary as long as the internal forces and moments are determined by linear methods. When non-linear analysis methods are used, additional checks of accumulated plastic deflections and repeated yielding will generally be needed. These checks are important in the case of variable or cyclic loading, e.g. wave loads. [3]

Due to different load cases, the structure is subjected to a variety of phenomena, which can be accounted for by the non-linear behavior. It also accounts for the possible interactions between those forces and phenomena, and this interaction may be difficult to formulate. Moreover, problems become non-linear when stiffness and loads become a function of displacement and deformation.

Those phenomena in structures may be material yielding, plastic strain local buckling of members, and holes in the geometry. Nonlinear problems induce the difficulty of describing phenomena by realistic mathematical and numerical models and the difficulty of solving nonlinear resultant equations. The effort required of the analyst increases substantially when a problem becomes nonlinear. Computational cost may also be a concern, despite the growing capability of computers[7].

Over the past decades, a significant amount of research has been carried on the development of ultimate limit strength formulations for buckling capacities. Paik et al. [8] derived sets of ultimate strength formulations for the steel plate elements that are under four load components such as compression/tension, edge shear, and lateral pressure loads. The study assumed that the plates are simply supported from all edges.

Cho et al. [8] used a simplified numerical method to detect the structural behavior under combined loads. A parametric study was then done using these methods to determine the ultimate strength of the stiffened plates under different cases of loading. A regression study of the results was used to find the ultimate strength formulations. The formulation provided acceptable results with DNV (Plate ultimate limit state) standard and ABAQUS predictions. The aim of Cho's study was to develop formulas that predict the ultimate strength of stiffened plates under the influence of combined axial compression, transverse compression, shear force, and lateral pressure loadings without the need to analyze the plate's non-linearly.

Ozguc et al. [9] introduced a simple design equation to calculate the buckling strength of stiffened panels taking into account both welding-induced residual stresses and geometrical

imperfections. Wide range ship panel geometries were investigated using non-linear finite element analysis to validate the equation's results.

Zhang [10] focused on panels under compression and developed a semi-analytical formula to predict ultimate strength capacity under axial compression (buckling capacity), Zhang also reviewed and validated the formula using different non-linear FE analysis models.

More recently, Ozguc [5] utilized the nonlinear finite element code ADVANCE ABAQUS, where an imperfection sensitivity work of a stiffened deck panel on an FPSO vessel is additionally accounted for. In-plane bi-axial compression in two orthogonal directions was explored in the cases studied. For the stiffened panels, the results are compared to the DNVGL PULS (Panel Ultimate Limit State) buckling code. The strength estimates from ADVANCE ABAQUS and DNVGL PULS code are found to be highly similar.

However, there is a need for more studies on achieving the calibration and compression of buckling capacities found using the non-linear methods and traditional buckling capacity standards. This is especially for complex geometry, such as a large ship hull stiffened where nonlinearities and geometry deformation are harder to predict and has a more significant effect on the buckling capacity.

2.2 Buckling capacity according to DNV-RP- C201

The NORSOK standard [2] is developed by the Norwegian petroleum industry to ensure adequate safety, value-adding and cost-effectiveness for petroleum industry developments and operations. It references Det Norske Veritas recommended practice DNV-RP-C201[1], Buckling Strength of Plated Structures, Part 1. for the design of plated structures such as stiffened panels.

The buckling capacity determined according to DNV-RP-C201[1] will be considered as a benchmark to calibrate the non-linear finite element model. When calibration is achieved, the nonlinear FE model can be used as basis for buckling capacity analysis where the geometrical properties of the panel are different from the cases within the limitations of the DNV-RP-C201[1] standard. This is after considering the assumptions made in the nonlinear analysis. The parameters that the DNV-RP-C201[1] takes into account when determining the buckling capacities are discussed in this section.

2.2.1 Design by LRFD method

LRFD method is a design method by which the target safety level is obtained as closely as possible by applying load and resistance factors to characteristic loads and resistance. The target safety level is achieved by using deterministic factors representing the variation in load and resistance and the reduced probabilities that various loads will act simultaneously at their characteristic values [11].

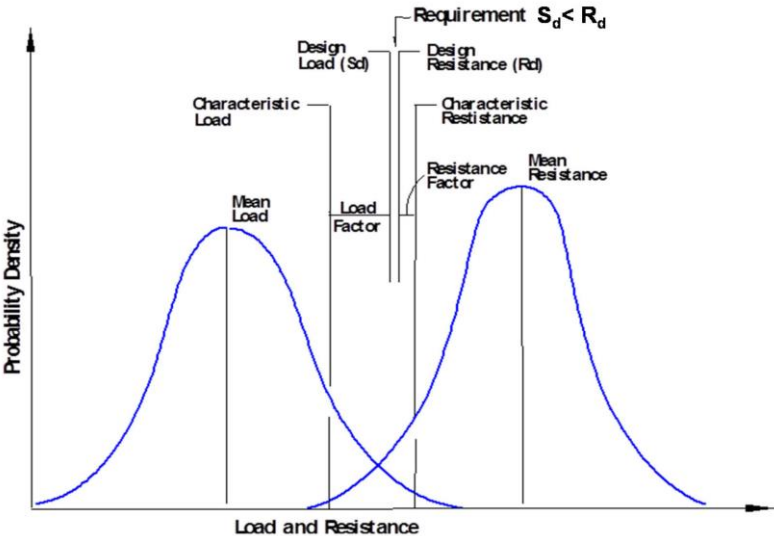


Figure 3-Illustration of the limit state safety format [3]

The level of safety of a structural element is considered to be satisfactory if the design load effect (S_d) does not exceed the design resistance (R_d) as shown in Figure 3:

$$S_d \leq R_d$$

Equation 2-1

Where the equation: $S_d = R_d$, defines a limit state

Characteristic load represents values for the different groups of limit states in the operating design conditions. For the ULS load combination, the representative value corresponds to a load effect with an annual probability of exceedance equal to, or less than, 10^{-2} (100 years). While the Characteristic resistance value which will imply that there is less than 5% probability that the resistance is less than this value. [11]

2.2.2 Ultimate limit state (ULS)

The ULS (also called ultimate strength) represents the failure of the structure due to a reduction of structural stiffness and strength. This is due to:

- Local or global structural equilibrium is generally considered rigid body (capsize, overturning).
- Reaching the maximum local or global structural resistance due to yielding or fracture.
- Structural component instability caused by buckling and plastic collapse

The simplified ULS depends on estimates of the structural component's buckling strength, commonly by using the elastic buckling strength after a simple plasticity correction- (Point A) in Figure 4. This is used when no detailed post-buckling behavior information is taken into consideration.

However, the location of the Ultimate strength point (point B) and whether it's under or above point A is uncertain when the post-buckling behavior and its interaction between the structural components are not considered. This caused difficulties to determine the real safety margin, making the design of structures such as ships, and platform etc., to increasingly rely on the ultimate strength limit (point B).

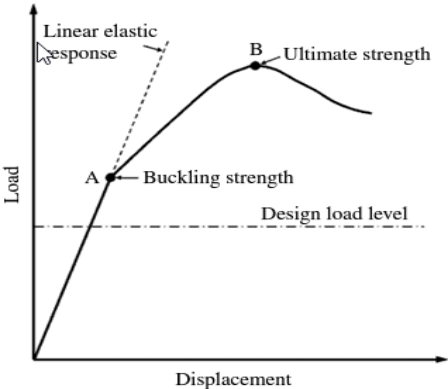


Figure 4-Structural design considerations based on the ultimate limit state[6]

The safety format of NORSOK requires structures to have ductile behavior. This results in a structure that does not have a sudden global collapse because ductility allows to redistribute internal stresses and thus absorbs greater amounts of energy before global failure

2.2.3 Stiffener type

The DNV-RP-C201[1] standard describes two types of stiffeners according to their structural function: (1) continuous and (2) sniped stiffeners.

Continuous stiffeners: These are connected to the frame and girders, so they contribute to the global strength with their full moment resistance, as demonstrated in Figure 5.



Continuous stiffener

Figure 5- Continuous stiffener [12]

Sniped stiffeners: These are disconnected, so when they intersect with the frame and girders, they form a simple support on the intersection point. Sniped stiffeners are considered only a stiffener stabilizing the plate fields between girder spans with no contribution to the global strength as shown in Figure 6.



Sniped stiffener

Figure 6-Sniped stiffener[12]

2.2.4 Buckling length

The buckling length of a continuous stiffener may be determined using the following equation:

$$l_k = l \left(1 - 0.5 \sqrt{\frac{P_{sd}}{P_f}} \right)$$

Equation 2-2



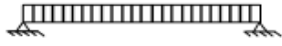
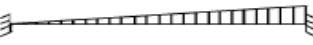
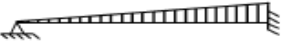

where,

P_{sd} : is design lateral pressure and P_f is the lateral pressure giving yield in outer-fibre at support.

2.2.5 Bending moment factors K_m

According to DNVGL-OS-C101 [13] Design of offshore steel structures, general- LRFD method, In Table 2 K_m values are given for defined load and boundary conditions.

Table 2- Bending moment and shear force factors K_m

Load and boundary conditions			Bending moment and shear force factors		
Positions			1	2	3
1 Support	2 Field	3 Support	k_{m1} k_{r1}	k_{m2} -	k_{m3} k_{r3}
			12 0.5	24 -	12 0.5
			- 0.38	14.2 -	8 0.63
			- 0.5	8 -	- 0.5
			15 0.3	23.3 -	10 0.7
			- 0.2	16.8 -	7.5 0.8
			- 0.33	7.8 -	- 0.67

2.2.6 Geometry

The geometry is of an idealized stiffened plate. It is characterized as having four corners labeled A-D and three stiffener points labeled 1 to 3. The plate length (L) is always more than or equal to the stiffener spacing. See Figure 7 below for definitions. [12]

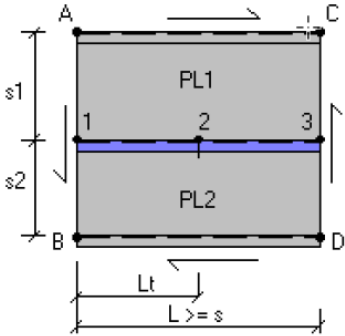


Figure 7- Idealized stiffened panel [12]

2.2.7 Buckling check procedure according to DNV-RP-C201 :

The DNV-RP-C201[1] standard requires the following checks to be fulfilled for continuous stiffened panels under axial compression loads and lateral pressure:

Eq 2-3 represents the buckling check for the stiffener at support in point 1 in Figure 7 which is where the compression stress is applied on the stiffener's side. If the applied design stresses are higher than the resistance design stresses equation 2-3 would be more than 1, UF(usage value)=1 and thus a buckling failure would be expected to happen in the stiffener at support point 1.

$$\frac{N_{Sd}}{N_{ks,Rd}} + \frac{M_{1,Sd} - N_{Sd} \cdot z^*}{M_{s1,Rd} \left(1 - \frac{N_{Sd}}{N_E}\right)} + u \leq 1 \quad \text{Equation 2-3}$$

Equation 2-4 represents the buckling check for the plate at support point 1. If equation 2-4 is more than 1, a buckling failure under the applied stresses would be expected to happen in the plate at support point 1.

$$\frac{N_{Sd}}{N_{kp,Rd}} - 2 \cdot \frac{N_{Sd}}{N_{Rd}} + \frac{M_{1,Sd} - N_{Sd} \cdot z^*}{M_{p,Rd} \left(1 - \frac{N_{Sd}}{N_E}\right)} + u \leq 1$$

Equation 2-4

where,

N_{Sd} design axial force

N_{Rd} buckling axial resistance

$M_{1,Sd}$ design bending moment at point 1

$N_{kp,Rd}$ design plate induced axial buckling resistance

$M_{st,Rd}$ design bending moment resistance on stiffener side in tension

N_E Euler buckling strength

z^* is the distance from the neutral axis of the effective section to the working point of the axial force. z^* is optimized in the equations to find the maximum resistance of the stiffened panel.

u is the design shear stress to the design resistance shear stress squared ratio

Equation 2-5 is a stiffener buckling check at mid-span (point 2)

$$\frac{N_{Sd}}{N_{ks,Rd}} - 2 \cdot \frac{N_{Sd}}{N_{Rd}} + \frac{M_{2,Sd} + N_{Sd} \cdot z^*}{M_{st,Rd} \left(1 - \frac{N_{Sd}}{N_E}\right)} + u \leq 1$$

Equation 2-5

where,

$M_{2,Sd}$ design bending moment at point 2

$M_{s2,Rd}$ design bending moment resistance on stiffener side at point 2

$N_{ks,Rd}$ stiffener induced design axial buckling resistance

Equation 2-6 is plate buckling check at mid-span (point 2)

$$\frac{N_{Sd}}{N_{kp,Rd}} + \frac{M_{2,Sd} + N_{Sd} \cdot z^*}{M_{p,Rd} \left(1 - \frac{N_{Sd}}{N_E} \right)} + u \leq 1$$

Equation 2-6

where,

$M_{p,Rd}$ plate side design bending moment resistance

$N_{kp,Rd}$ design plate axial buckling resistance

2.3 Non-linear buckling capacity according to DNV-RP-C208

Nonlinear problems pose the difficulty of describing phenomena by realistic mathematical and numerical models and the difficulty of solving nonlinear equations. The effort required of the analyst increases substantially when a problem becomes nonlinear. Computational cost may also be a concern, despite the growing capability of computers.[7]

Problems become non-linear when stiffness and loads become a function of displacement and deformation, in buckling structures, nonlinearity include the following:

- Material nonlinearity: where material properties are functions of stress strain relation, including the elastic, plastic, and creep phases.
- Contact nonlinearity, in which a gap between adjacent parts may open or close, the contact area between parts changes as the contact force changes, or there is sliding contact with frictional forces.
- Geometrical nonlinearity: when the displacement and the alteration in the geometry become large enough to influence the equilibrium equations so that they must include the deformed geometry. In addition to loads, directions that might change as they increase and the geometry deform. [7]

For buckling analyses, it is necessary to introduce equivalent geometric imperfections in order to predict the buckling capacity correctly. This will be discussed further in the next chapters.

The DNV-RP-C208[3] recommended practice provides guidance on establishing structural buckling resistance using the non-linear finite element method. It is concerned with identifying the characteristic resistance of a structure or section of a structure to meet the DNV criteria for ultimate strength in DNV recommended practices DNV-RP-C201[1].

The non-linear buckling analysis according to DNV-RP-C208 [3] is not intended to replace the determination of structural buckling resistance according to traditional standards but to cover the cases that are not within the limitations of the standards.

When using FE methods to analyze buckling resistance, it is critical to account for the statistical variation of the different parameters. This is done so that the results reflect a safe estimate when compared to the results acquired, if physical testing could be performed. When the statistical variance is uncertain, the best engineering judgment must be applied to choose the regulating parameters.

The parameters should be set so that the established characteristic resistance may be justified as fulfilling the requirement of the capacity being 5% likely to be less than this value complying with the ultimate limit state.

For this reason, DNV-RP-C208 [3] recommends three validation methods for the non-linear analysis:

- All controlling parameters should be set to characteristic or conservative values where the key parameters such as element, mesh size, imperfections, and material curve are selected to be on the safe side.
- Validation against design standards values, where a standard case that represents the same failure mode is utilized for calibration. The key parameters are selected so the non-linear analysis results in the resistance capacity calculated according to the standard. Those parameters are then used to determine the resistance of the actual case to be investigated. This method will be used to investigate the stiffened panel model in this thesis.
- Validation against test where one or more physical tests for calibration that are deemed to fail in a compatible fashion to the problem to be investigated (denoted test calibration case). To begin, critical factors such as element type, mesh size, material curve, defects, residual stresses are modified to ensure that the analysis accurately replicates the test calibration situation (providing the same amount of resistance or less). The actual problem is then examined using the same key parameters. However, with regard to the problem at hand in this thesis and due to the high amount of time and resources that this method requires, the validation against buckling capacities determined by the standards, are used to validate the results of the non-linear buckling analysis of the stiffened panel.

Chapter- 3 Establishing benchmark buckling capacity according to DNV-RP-C201

The buckling capacity according to DNV-RP-C201[1] is determined using STIPLA DNVGL program, which is developed to determine the buckling strength of plated structures using DNV-RP-C201[1] checks and criteria.

3.1 Safety format

The safety format used in the analysis is LRFD and since $Sd = Rd$, it defines a limit state. The characteristic resistance should reflect a value with a less than 5% chance of the resistance is less than this value. Because a lack of experimental data frequently prevents an adequate statistical evaluation, the 5% probability level should be regarded as a target when engineering judgements to be made. For this reason, it is assumed that the uncertainties in the material resistance for this model are adequately addressed when the characteristic resistance is used to determine the characteristic calibration buckling capacity for the non-linear model. Thus, the material factor in STIPLA, used for the calibration benchmark, is chosen as $Y_m=1$, and the usage factor=1.

3.2 Stiffener type and geometry

the stiffeners are chosen as continuous stiffeners in STIPLA in order to calibrate the finite element model, where the stiffeners are connected and continued through the girders and contribute with their full moment capacity to the buckling strength.

The bulb flat stiffener profile is transformed to an L-profile with the same area as the area of stiffener in the file. The L-profile was chosen so the cross-section closely matches the actual bulb profile in I_y - and I_z - and Area. The geometry of the converted profile is shown in Table 3 and in Figure 8 [12]:

Table 3-Stiffener geometrical properties

Stiffener geometrical properties	Dimensions
H	240 mm
Tw	10 mm
C	34 mm
r	10 mm
B	39,5 mm
Tf	28,8 mm
G	25,5 kg/m
Ax	3249 mm ²

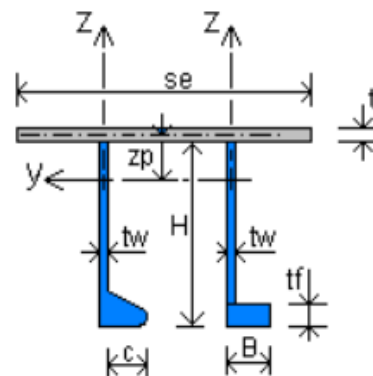


Figure 8-Geometrical properties of stiffeners [12]

3.3 Buckling length and bending moment factors K_m

P_f is the lateral pressure giving at support, P_{sd} is chosen as 0,002 to account for gravity load. The buckling length $L_k=3758\text{mm}$. According to eq2.2

The support conditions are considered fixed, so the Moment factors as chosen as $K_{m1}=12$
 $K_{m2}=24$ from Table 2.

3.4 Geometry and material properties

Geometry is as shown in the following Table 4- Panel geometry and the geometrical properties chapter. lateral-torsional buckling length is equal to the stiffener span.

Table 4- Panel geometry

Geometry	
Stiffener span L	3800 mm
Length of girder L_g	16000 mm
Plate thickness t	15 mm
Stiffness spacing S1, S2	800 mm
Lateral torsional buckling length L_t	3800 mm

The material properties for the plate, stiffener and girder are chosen according to VL/DNVGL-OS-B101. The yield strength is $F_y=235\text{MPa}$, Young's Modulus of elasticity is $E=2,1\text{E}+5 \text{ MPa}$, Poisson's ratio=0,3.

3.5 Applied stresses

It is preferred to reduce the uncertainties related to combined loads buckling capacity analysis since compression loads are the governing loads in buckling strength analysis. Only uniaxial in-plane compression stress in the stiffener direction (X) and pressure load P_{sd} as shown Figure 9 $\sigma_A = \sigma_B$. While stresses in the Y direction (σ_y), and Shear(T) are chosen to be zero in the calibration and the non-linear model. The loads applied to the model are shown in Figure 9

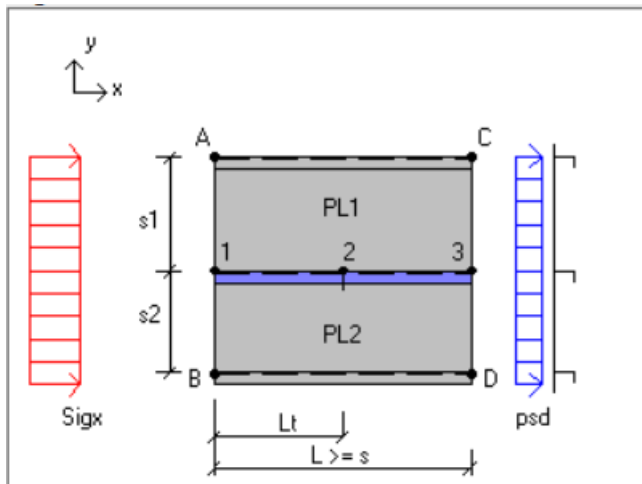


Figure 9- Applied loads in buckling capacity according to DNV-RP-C201[1]

3.6 Buckling check results according to DNV-RP-C201

Compression stress is applied on plate boundary alone stiffener as $\sigma_A = \sigma_B = 0$ MPa and increased 10 MPa in each step while applying a constant 0,002 MPa as a gravity lateral pressure on the plate side of the panel using eq 2-3, 2-4, 2-5, 2-6 to produce lines UF1s, UF1p, UF2s, UF2p respectively. This results in Figure 10 for lines UF1s and UF1p, Figure 11 for lines UF2s and UF2p, where each compression stress is corresponding with a usage value (UF), the compression stress that corresponds with a usage value of 1 in any of the four buckling check lines is chosen as a calibration value for the non-linear analysis.

As shown in Figure 10, which includes lines UF2p, UF1s have close buckling behavior under the increasing buckling load. Since both lines reach one at compression load 170 MPa, buckling would be expected under compression load of 170 MPa at point 1 near the support location of the stiffeners and point 2 in the middle of the plate.

Whereas, in Figure 11 the lines decrease to negative values under the applied compression stresses. This is due to the nature of equations 2-5, 2-6 that are found using experimental and analytical data. Thus, no buckling would be expected at the support location of the plate point 1, and at the middle of the stiffeners at point 2 under the compression load 170 MPa.

Performed checks according to DNV-RP-C201[1], (Appendix)

- plate and stiffener yield check.
- plate under lateral pressure check.
- Plate thickness check.
- Stiffener section modulus check according to DNVGL-OS-C101 (Ch.2. Sec.4).
- Girder buckling.

They all pass the required criteria in the standards under both compression stress 170 MPa and $P_{sd}=0,002$ MPa stresses.

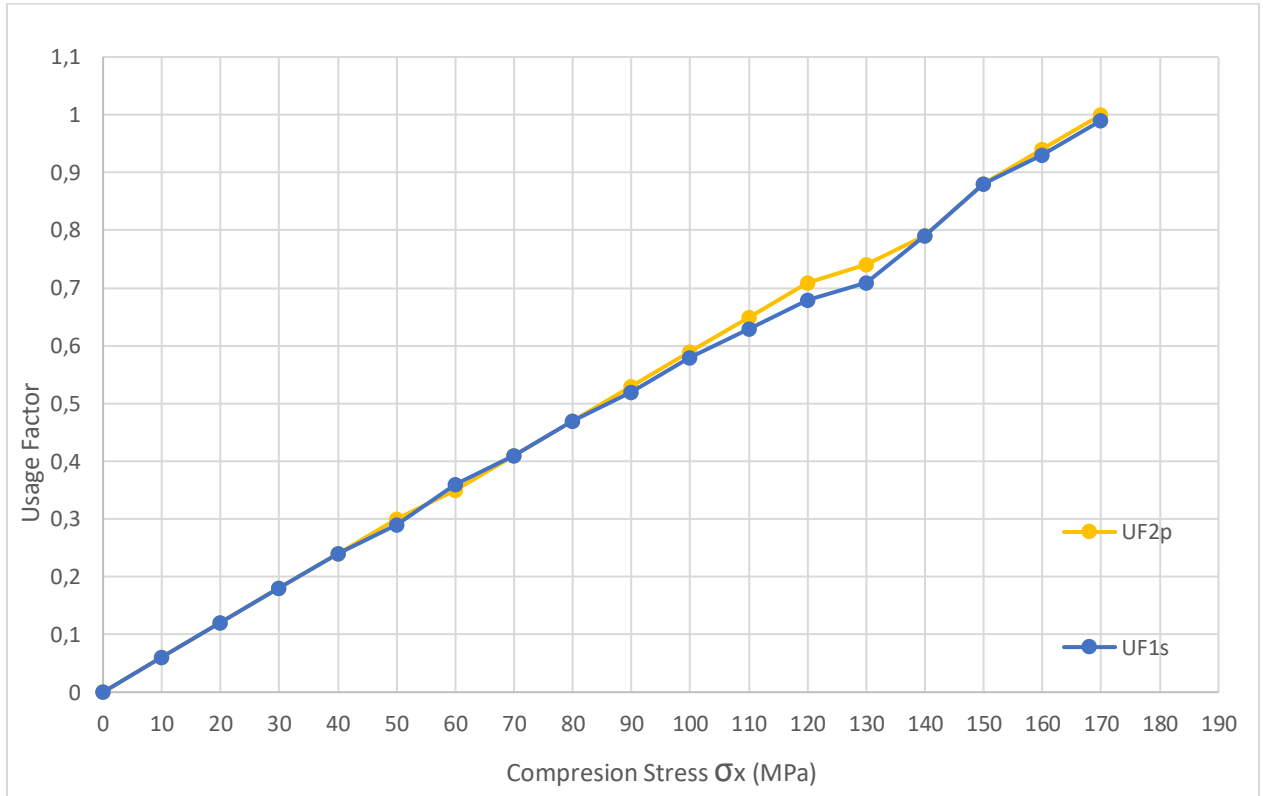


Figure 10-Plate-Stiffener buckling ccheck-1

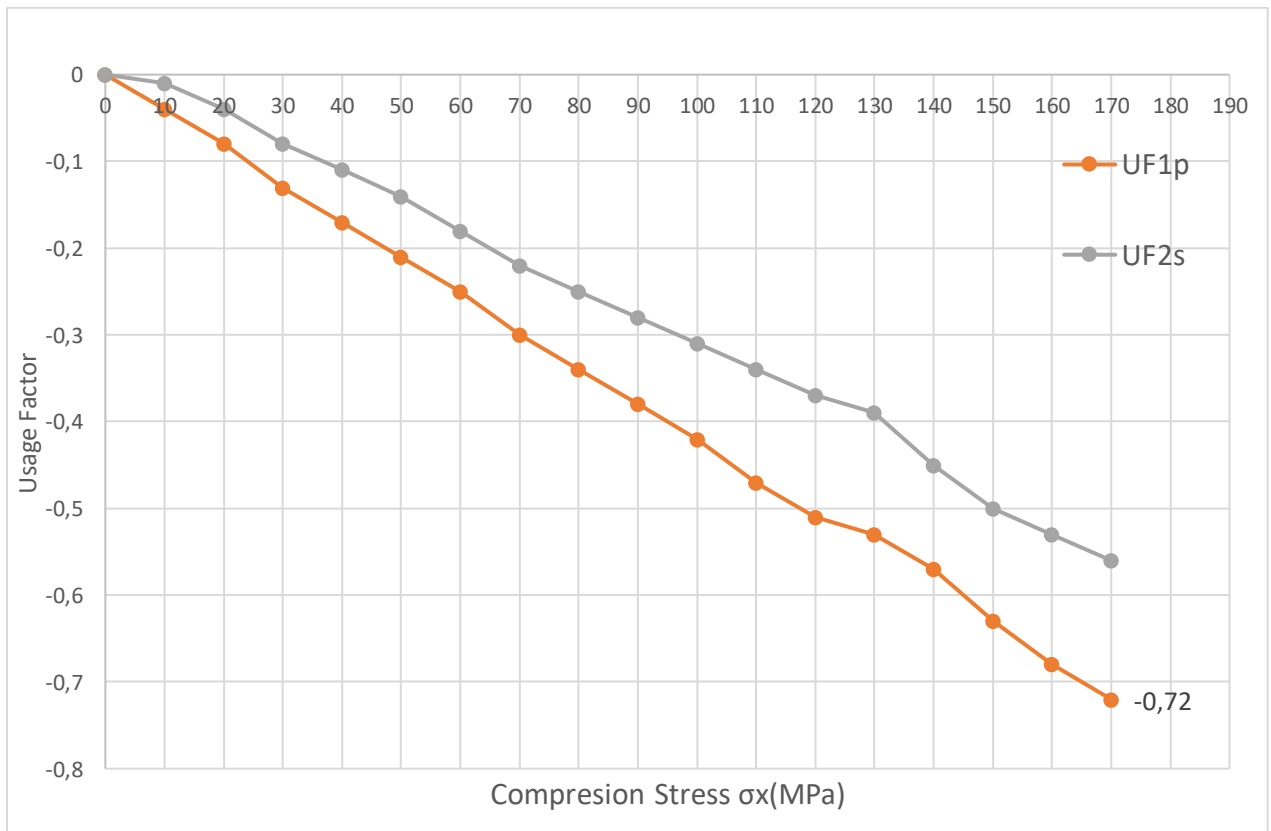


Figure 11-Plate stiffener buckling check-

Chapter- 4 Finite Element Model Description of Ship Hull Stiffened Panel

4.1 Geometrical properties

The stiffened panel investigated is an idealization of the ship hull panel in Figure 12.

The FE model consists of a rectangular panel with 19 equally spaced bulb flats stiffeners and three equally spaced girders, and geometrical properties are of a commonly used stiffened ship hull panels in the North Sea as demonstrated, the dimensions of the plate, stiffeners and girders are given in Table 5.

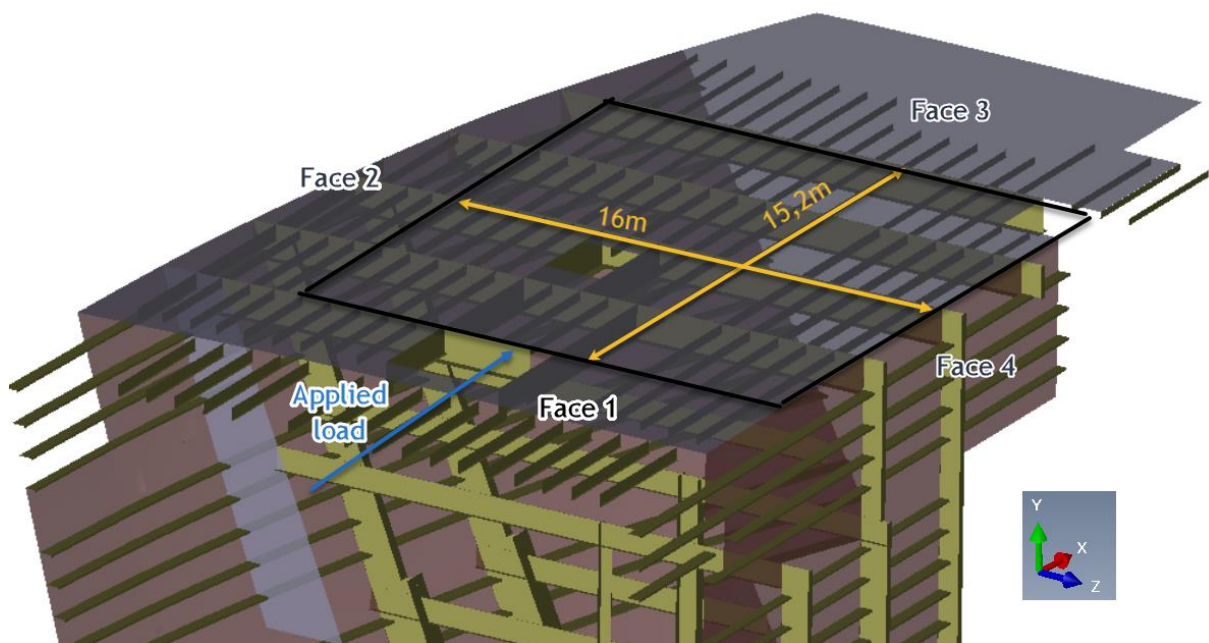


Figure 12- Real ship hull stiffened panel model

Table 5- Geometrical properties of FE model

Plate	
Plate thickness	15mm
Plate length	16000mm
Plate width	15200mm
Stiffeners geometrical properties	
Profile type	Bulb flats
Number of stiffeners	19
Stiffener length	15200 mm
Stiffener Span	3800mm
Stiffener spacing	800mm
Stiffener height (including flange thickness)	240mm
Stiffener web thickness	10mm
Stiffener Bulb width	39,5mm
Stiffener Bulb thickness	28,8mm
Girder geometrical properties	
Profile type	Girder T
Number of Girders	3
Girder length	16000mm
Girder spacing	3800mm
Girder web height (including flange thickness)	930mm
Girder web thickness	12,5mm
Girder Flange width	450mm
Girder Flange thickness	30mm

4.2 Non-linear Material properties

S235 is widely used for the design of stiffened panels in ship hull. For this reason, S235 is chosen as the material for the stiffeners, plate, and girders. The non-linear material properties are chosen as DNV-RP-C208 recommends; all stresses used to represent true stresses as shown in Figure 13. The material properties are given in Table 6.

Table 6- Non-linear material properties

Thickness [mm]	$t \leq 16$
E [MPa]	210000
σ_{prop} [MPa]	211,7
σ_{yield} [MPa]	236,2
σ_{yield2} [MPa]	243,4
ϵ_{p_y1}	0,004
ϵ_{p_y2}	0,02
K[MPa]	520
n	0,166
σ_{UTS} [MPa]	326,925203

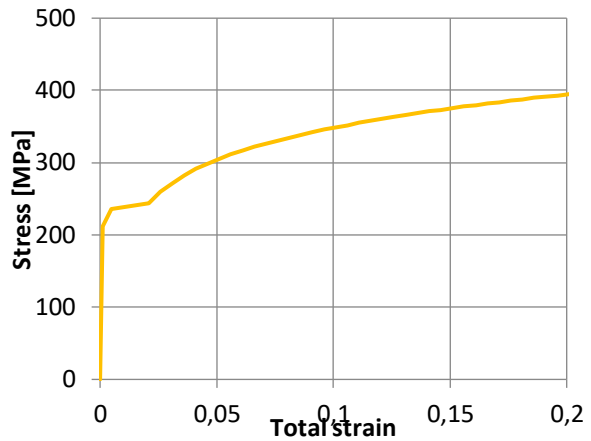


Figure 13-Non-linear material properties- stress-strain relation

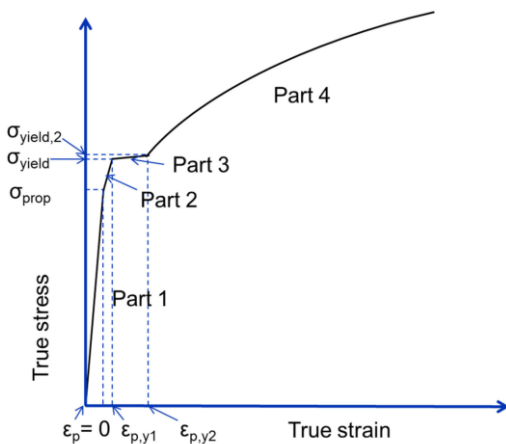


Figure 14-Non-linear material stress-strain relation

the stress-strain relation is explained in Figure 14

Part 1: the linear plastic behavior.

Part 2: Represents the stresses between the highest stress in the elastic regime and the initial yielding stress

Part 3: The yield plateau (plastic behavior).

Part 4: Represent the strain hardening (plastic behavior), the stress-strain relation is given by equation: [3]

$$\sigma = K \left(\epsilon_p + \left(\frac{\sigma_{yield\ 2}}{K} \right)^{\frac{1}{n}} - \epsilon_{p,y2} \right)^n \quad \text{for } \epsilon_p > \epsilon_{p,y2}$$

Equation 4-1

4.3 Applied force

As demonstrated in Figure 12, the force is applied on a reference point constrained to Face 1's nodes with kinetic coupling constraint. That is all nodes and the reference point of Face 1 would have equal displacements in all directions, and the force applied to the reference point would be equally distributed to each node in Face 1. Face 3 nodes are also constrained to RP-3 to measure the reaction forces of Face 3. The applied force is equal to the calibration stress acquired from DNV-RP-C201[1]. This stress is multiplied by the area of Face 1 (plate and stiffeners cross-sectional area). The applied force becomes $F_x=51296$ KN.

4.4 Boundary conditions

Since the panel is an idealization of the model in Figure 15, The boundary condition constrains are shown in the FE model in Figure 16 and in Table 7.

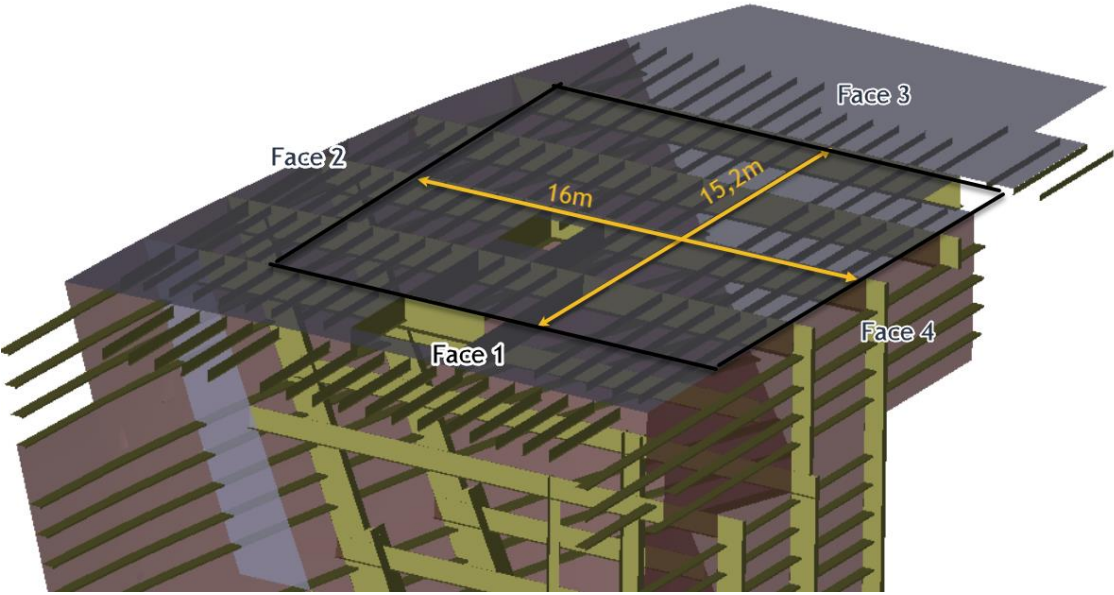


Figure 15- Real Ship hull stiffened panel boundary conditions

Table 7- FE model boundary conditions

	Constrained degree of freedom
Face 1	Y, Rz
Face 2	Y, Rx, Ry, Rz
Face 3	X, Y, Rx, Ry, Rz
Face 4	Y, Z, Rx, Ry, Rz

Since the force is assumed to be applied on Face 1 in the x-axis direction, the displacement is free in that direction. It is also free in Z direction to allow for the plate to have a displacement similar to Poisson's ratio deformation when the load is applied in the X-direction. Displacement

in the Y direction is constrained to prevent out-of-plane displacement of the plate and ensure that the load is fully distributed in the X-direction. The plate is assumed to be welded to a girder on Face 1 so it is constrained on Rz.

Face 2 is assumed to be fixed since it is connected to pillars and vertical plates. However, it is assumed to be free to move in the X direction to allow for buckling load-displacement in the X direction. And it is free for displacement in the Z direction to allow for Poisson's ratio deformation shape.

Face 3 is also assumed to be fixed since it is connected to a girder and horizontal plates, but displacement is allowed in the Z direction to allow for Poisson's ratio deformation of the plate.

Face 4 is assumed to be fixed since it is connected to pillars and vertical plates. However, it is free for displacement in the X direction to allow for displacement in loading direction.

Face 1 and Face 3 are constrained by kinetic coupling to reference points RP1 and RP3, and the boundary conditions are applied to the points.

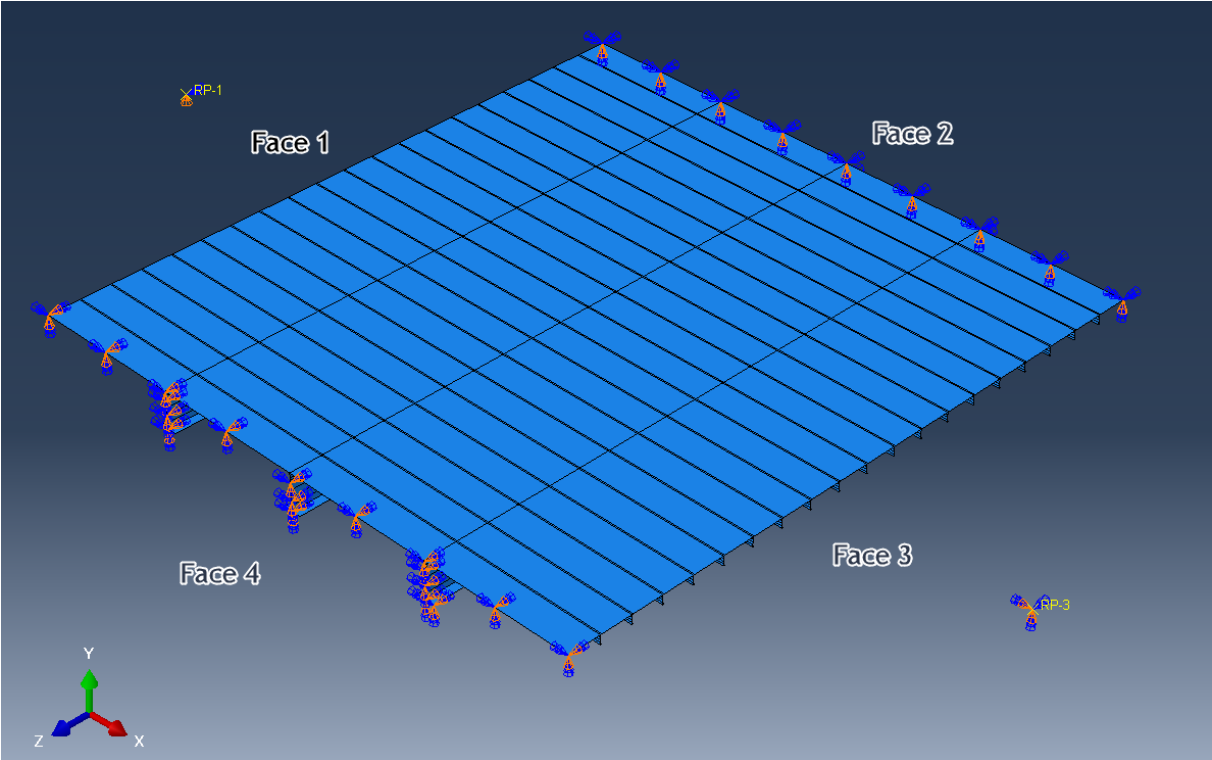


Figure 16 FE-model boundary conditions

Chapter- 5 Non-linear Finite Element Analysis of Stiffened Ship Hull Panel

5.1 Introduction and Assumptions

A non-linear buckling analysis using ABAQUS load-deflection (Riks) analysis is performed, where the effect of geometrical imperfection and material nonlinearity is accounted for.

Assumptions in the non-linear analysis:

- 1- the panel is perfectly constructed before applying the geometrical imperfections.
- 2- Stiffeners are straight and continuous through the girders, participating with their full moment capacity on the stiffeners- girders crossing point.
- 3- No buckling in the girders since the compression stress in the stiffener's direction. Girder's function is only to reduce the buckling length of the longitudinal stiffeners.
- 4- The non-linear analysis assumes a perfect contact and stress distribution between the different panel components.
- 5- Since compression in the stiffeners and plate are the governing load case for the buckling simulation at hand, only compression and gravity load are applied, no other load cases such as transverse and shear load are investigated or applied to the non-linear finite element model.

5.2 Element type

Linear quadrilateral shell element S4R is used. Shell elements are used because when using the Cartesian coordinate system, it makes it easier to specify the membrane stress components within each element. Moreover, the nodes of the shell element are located at the mid-thickness of each element resulting in no element mesh assigned to the thickness layers. [6]

5.3 Mesh size

The mesh was generated using the auto meshing tool ABAQUS provides. Some lines were added to the geometry to help the auto meshing tool to provide a more continuous mesh with fewer element transition irregularities.

As demonstrated in Table 8 and Figure 17, a mesh sensitivity study was performed on the model to decide on an acceptable mesh size regarding the required computational power and accuracy of the stress concentration in the mesh. The sensitivity study is done on 5 different mesh samples.

Table 8- Mesh sensitivity- element size assessment

	Mesh element number	Max nodal stress (MPa)	Increase in mesh size	Increase in max stress
Mesh 1	11418	163,571		
Mesh 2	25684	163,465	225 %	-0,06%
Mesh 3	49703	164,536	194 %	0,65%
Mesh 4	154000	172,355	310 %	4,5%
Mesh 5	437328	177,73	284%	3%

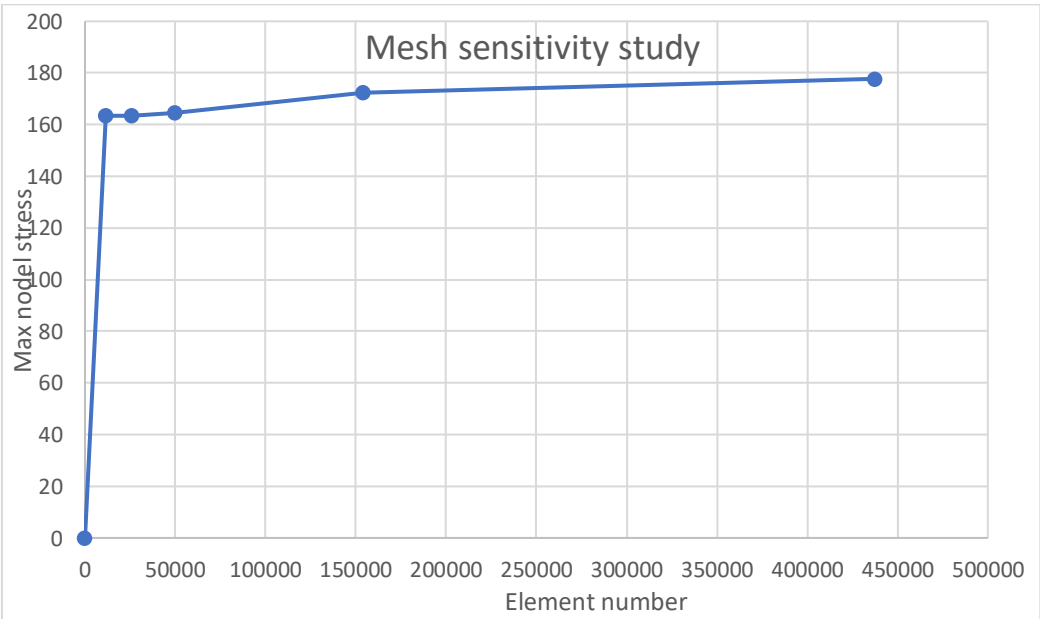
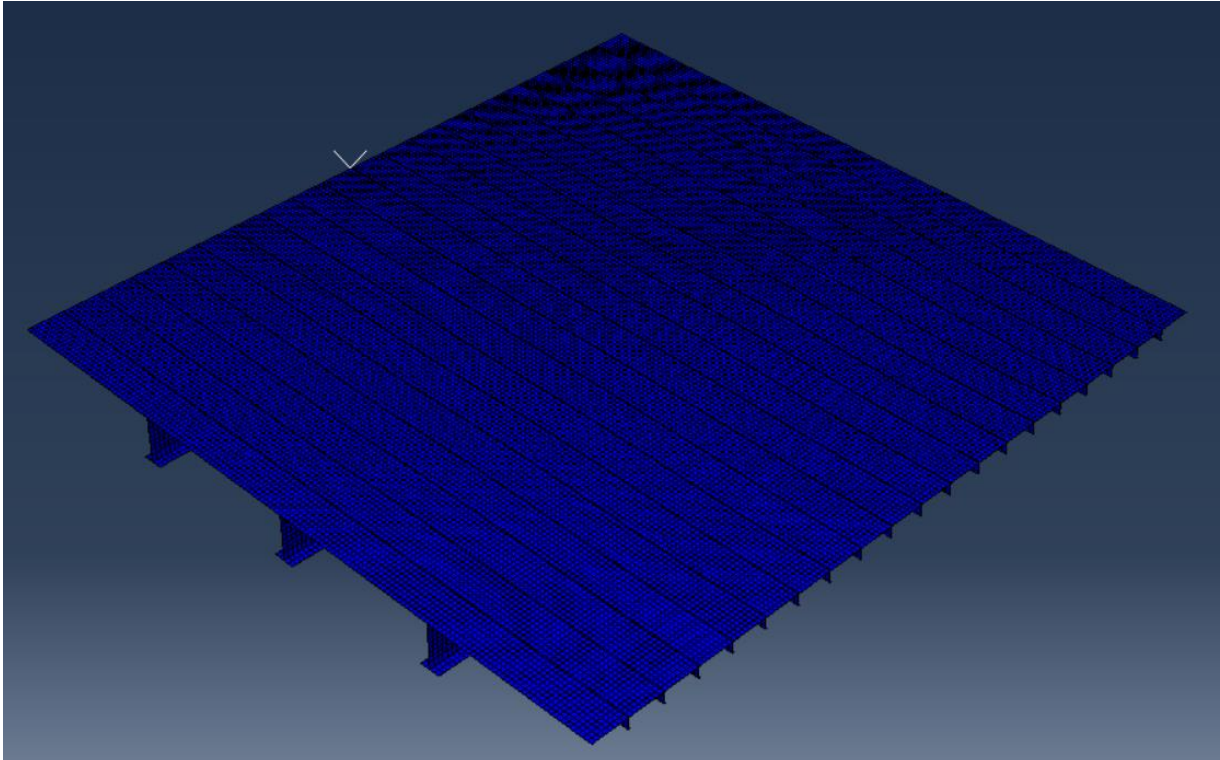
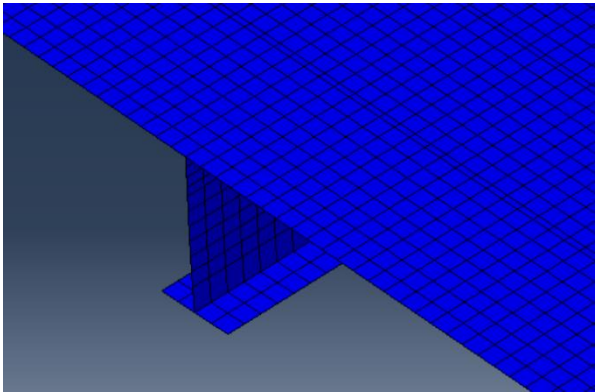


Figure 17-Mesh sensitivity study

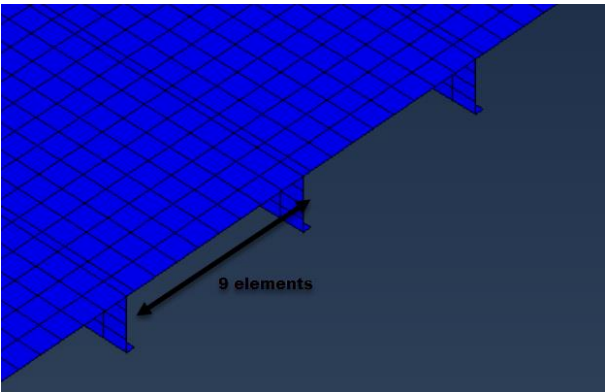
Mesh 3 with 49703 element is chosen for the analysis since a 310 % increase of the element number in the mesh would only lead to 4.5% increase in the maximum nodal stress in the panel. This will help reduce the computational cost required to analyze the panel non-linearly while having a sufficient level of accurate capacity [6]. In addition to the fact that at least 8 four-noded shell elements are required to plate mesh in between stiffeners, and mesh 3 has an average element aspect ratio of 1.45 which is close to the recommended value of unity. As shown in Figure 17, mesh 3 is compatible with the criteria mentioned.



(a) Panel mesh



(b) Girder mesh



(c) Stiffener mesh

Figure 18- Mesh-3 used in the FE non-linear model

5.4 Introducing the Geometrical Imperfection to the model

Geometrical imperfections are an important factor in determining the buckling strength of the structure. This is due to the fact that the resistance of plate structures is dependent on imperfections in several elements. However, it is less likely that all the elements have their highest imperfection pattern and size simultaneously. In the case of low slender plates, the importance of imperfections is at its highest. For this case, the reduced slenderness λ is 1.04 and the buckling factor is $k=0,76$, which means according to Figure 19 that the buckling capacity is more sensitive to geometrical imperfections. The reduced slenderness λ and buckling factor k are calculated according to DNV-RP-C208[3].

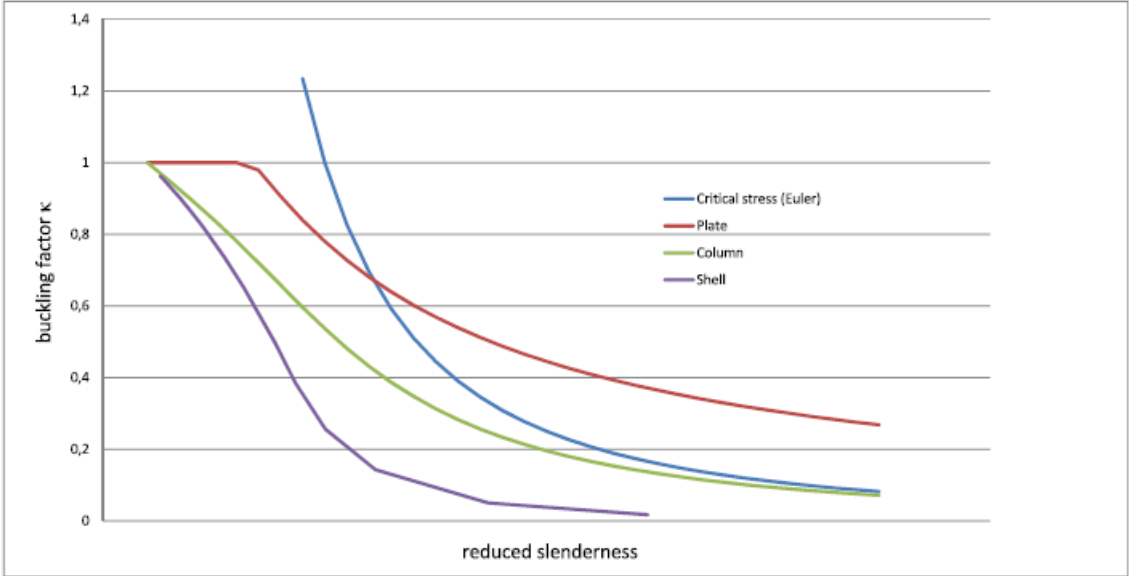


Figure 19-Examples of buckling curves showing sensitivity for imperfections etc. for different forms [3]

DNV-RP-C208[3] recommends that an eigen mode analysis of the panel to produce geometrical imperfection patterns. The recommended imperfections patterns (Figure 21) are divided into local and global imperfections, where local imperfections represent the imperfection pattern and amplitude for plane plate between stiffeners. Global imperfections however are on the longitudinal stiffener between girder webs direction. The recommended imperfection amplitude is shown in Table 9.

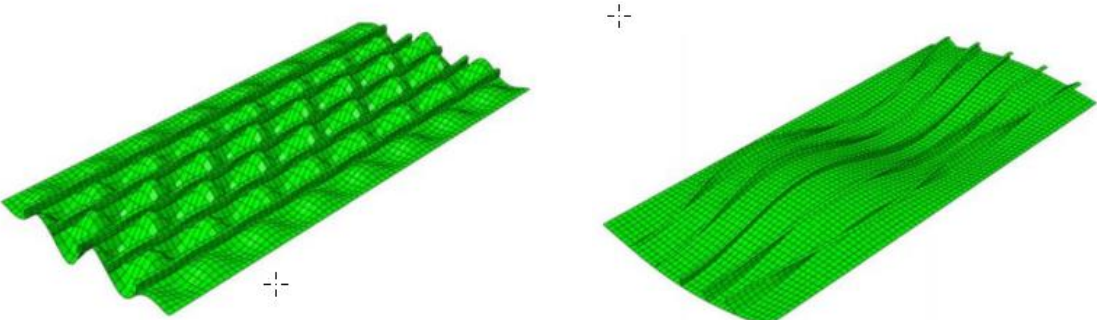
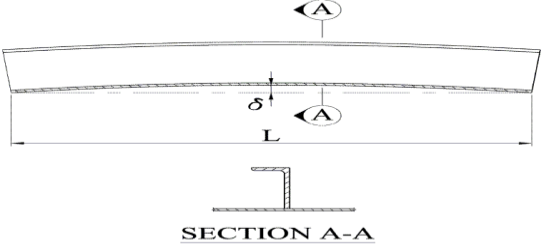
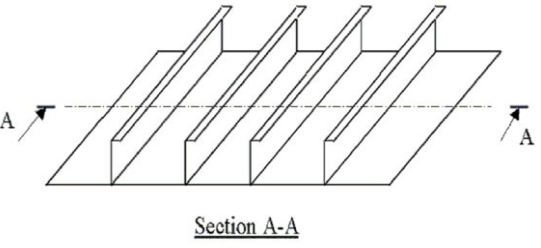


Figure 21 DNV-RP-C208 recommended Local Imperfection pattern (left), global Imperfection pattern (right)

Table 9- DNVRP-C208 imperfection amplitude recommendation [3]

Component	Shape	Magnitude	Imperfection amplitude	
Longitudinal stiffener girder webs (global imperfection)	Bow	$L/400$	4 mm	
Plane plate between stiffeners (Local imperfection)	Eigenmode	$S/200$	9.5 mm	

For this case, according to DNV-RP-C208 [3] at the combined (local and global) imperfection location, the amplitude would be 13.5 mm.

Imperfections are introduced to the model by perturbations in the geometry, to define the imperfections, linear superposition of multiple eigenmodes is performed. An eigenmode analysis is performed on the ideal structure. ABAQUS imports imperfection based on the superposition of weighted mode shapes. The displacements of the nodes from the eigenmode value are multiplied by scale factor to determine the magnitude of the nodes coordinate alteration that would provide the desired geometrical imperfection for the non-linear analysis model. [14]

5.5 Eigenmode analysis

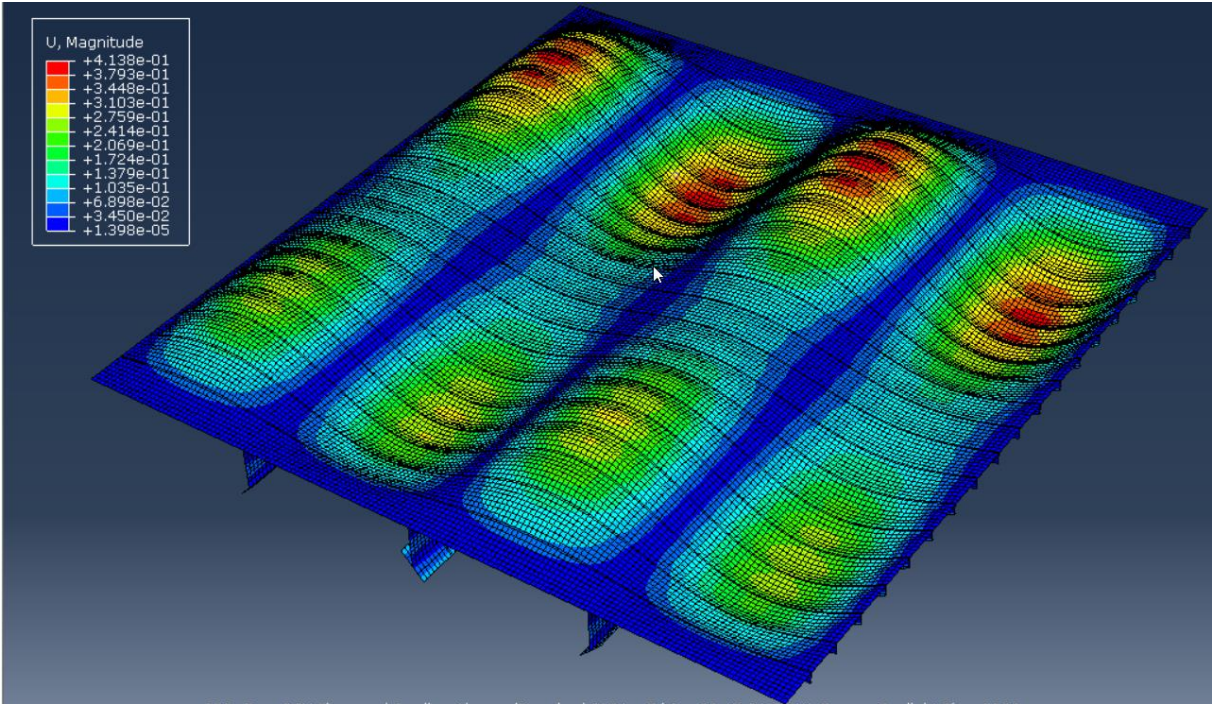
Since eigen mode analysis purpose is only to acquire the imperfection patterns recommended by the DNV standard C208[3], a different set of boundary conditions than those from the original model are applied to the eigen mode analysis.

The different boundary conditions provided eigen modes with patterns closer to the patterns recommended by DNV-RP-C208 [3] than the original boundary condition of the model.

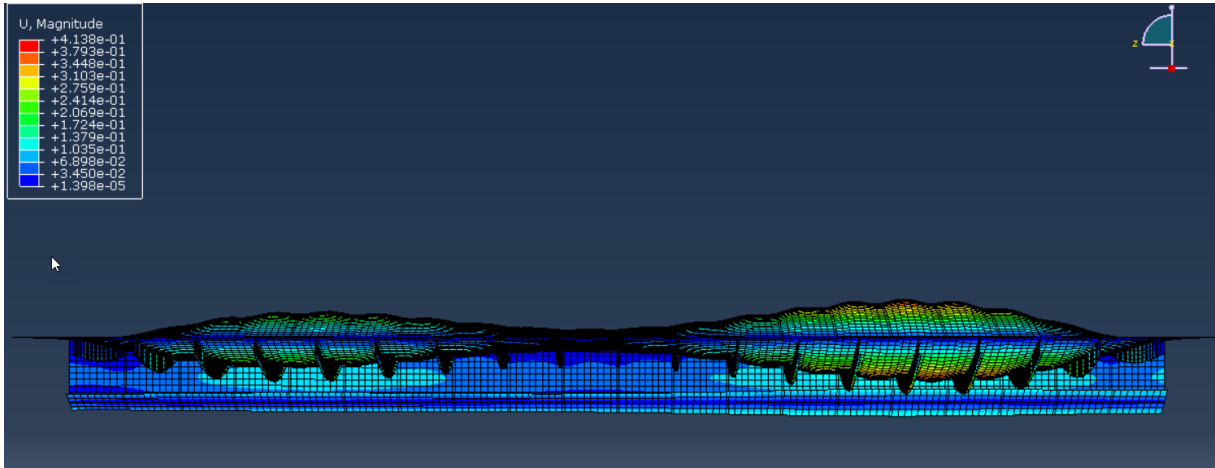
Eigenmode analysis is done using ABAQUS program, and 3 eigen modes patterns are investigated as imperfections in two different cases to determine the imperfections pattern and magnitude that will give result of the calibration benchmark buckling capacity.

Pattern of the global imperfection is as shown in Figure 22. The global imperfection patterns are the same for both cases. This pattern represents the closest global imperfections patterns in the eigenmode analysis. It represents the curved bow shape along the stiffener in between the girders.

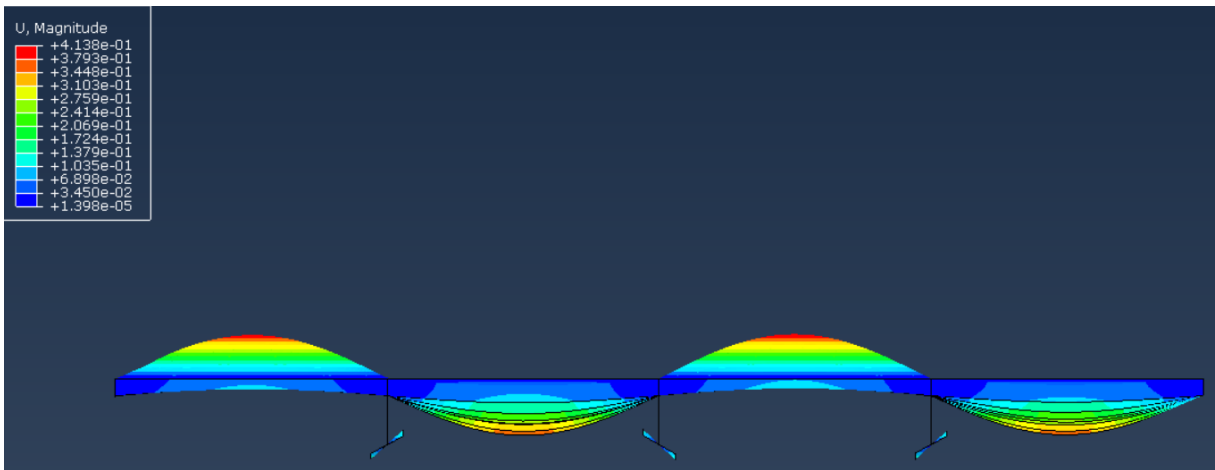
However, the magnitude of displacement is not equal at each mid-stiffener span along the panel, a displacement average amplitude value is determined at the middle of the relevant spans showing the maximum and minimum displacements of the relevant spans this also helps to represent a more realistic case of global geometrical imperfections magnitude and distribution.



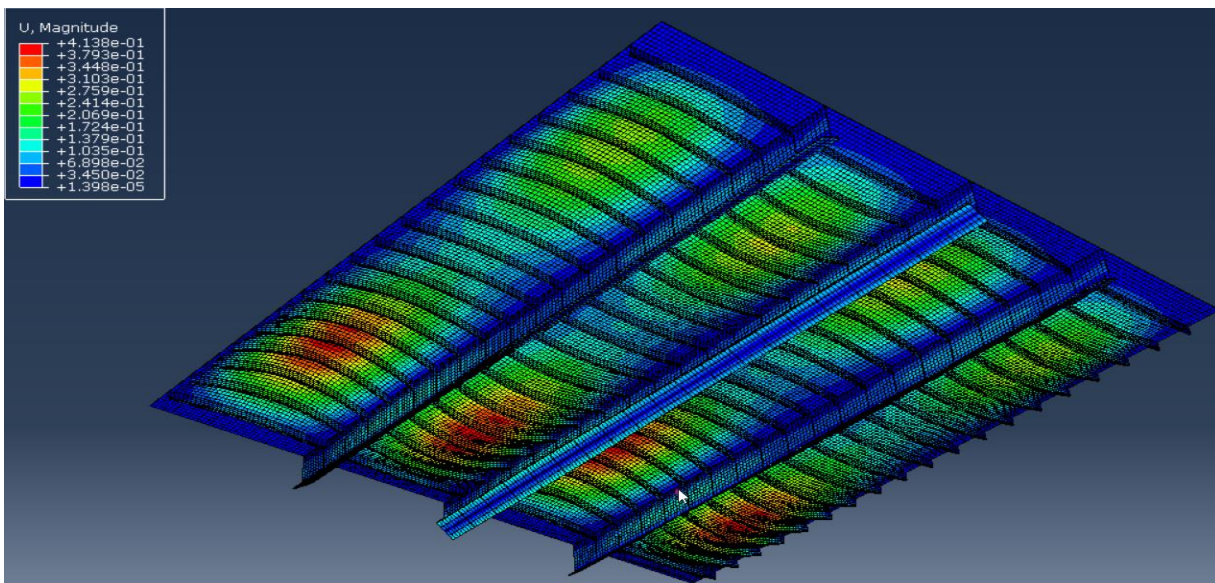
(a)Plate



(b) Stiffener side view



(c) Girder side view



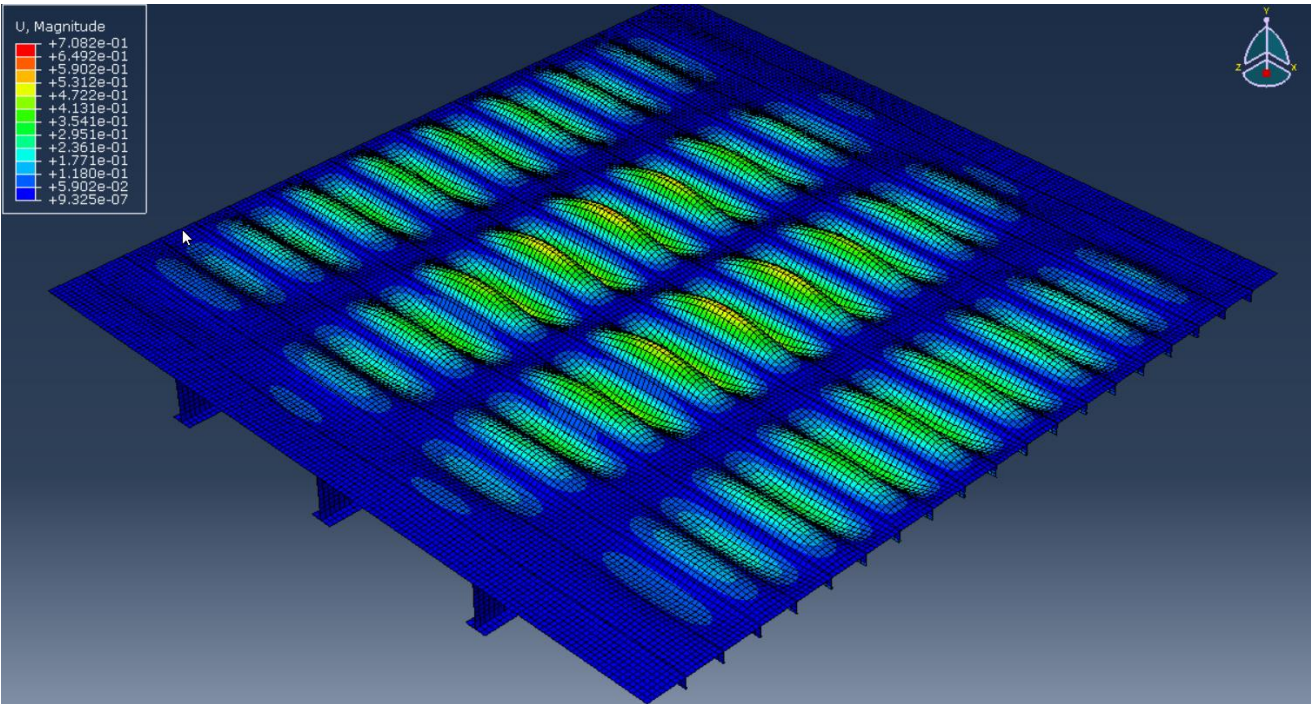
(d) Bottom view

Figure 22- Global imperfection pattern

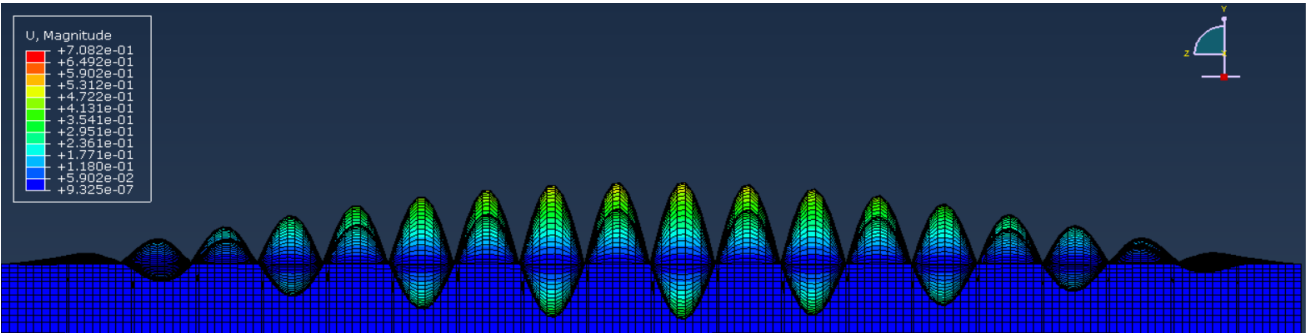
The local imperfection patterns, which are represented in Figure 23, show the displacement magnitude in the eigenmode of the nodes in the middle of the plate between the stiffeners. the unequal displacement would represent a more realistic local imperfection distribution.

the difference between the two patterns is shown in Figure 23 and Figure 24 where pattern 1 shows a sine shaped displacements with the displacement changing to the opposite direction in every sequential stiffener span.

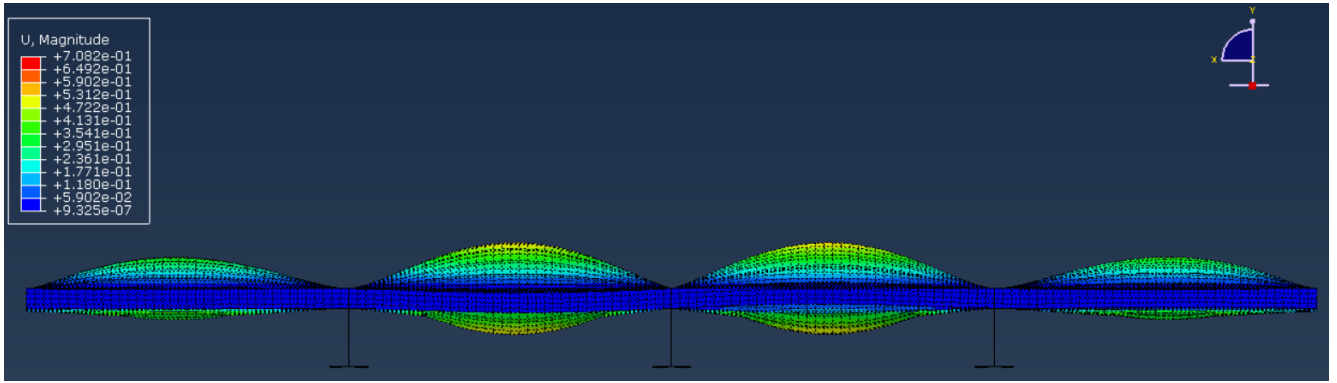
While in pattern 2 -in Figure 24- the displacement change direction in every two sequential stiffener span so that the first two stiffener spans have an opposite displacement direction from the last two stiffener spans.



(a) Plate

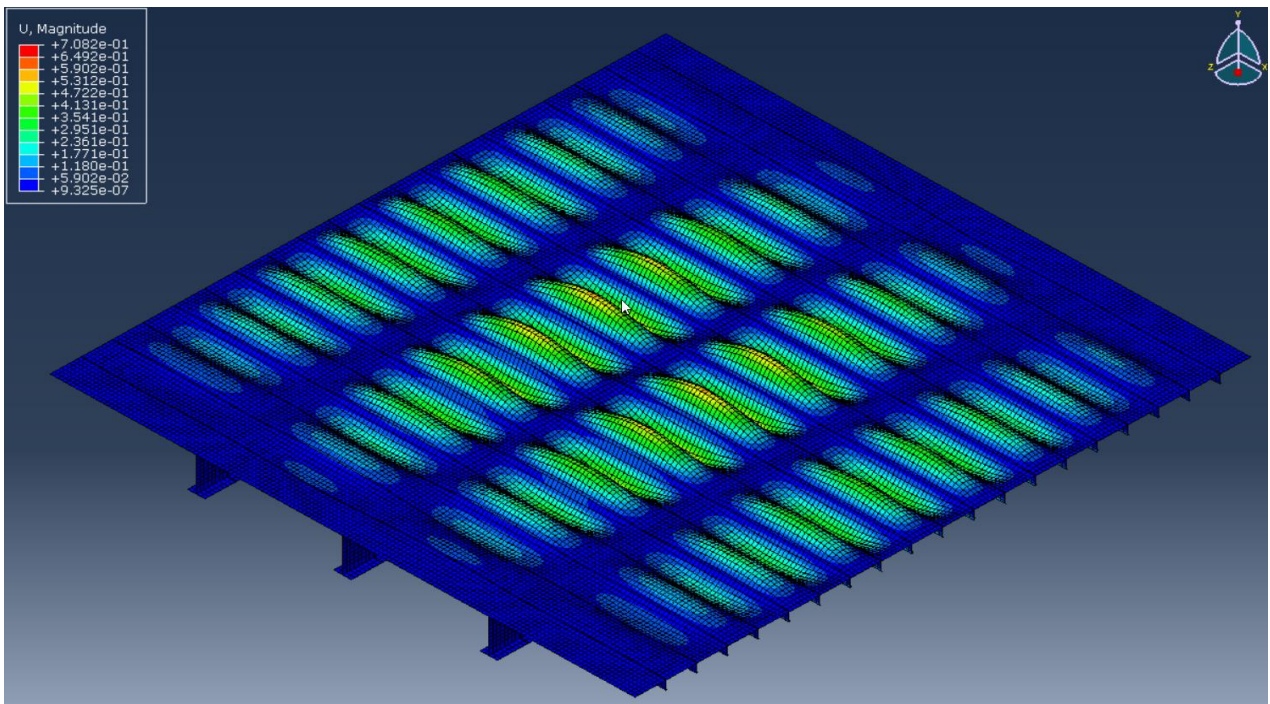


(b) Stiffener sideview

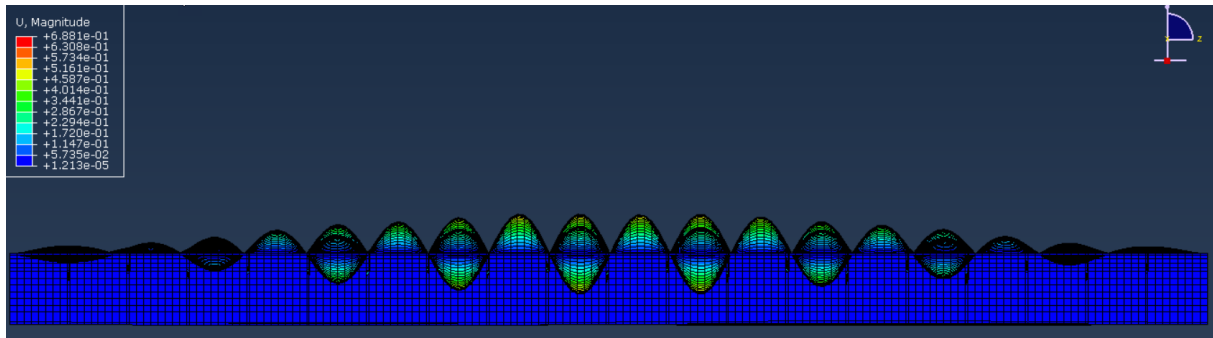


(c) Girder side view

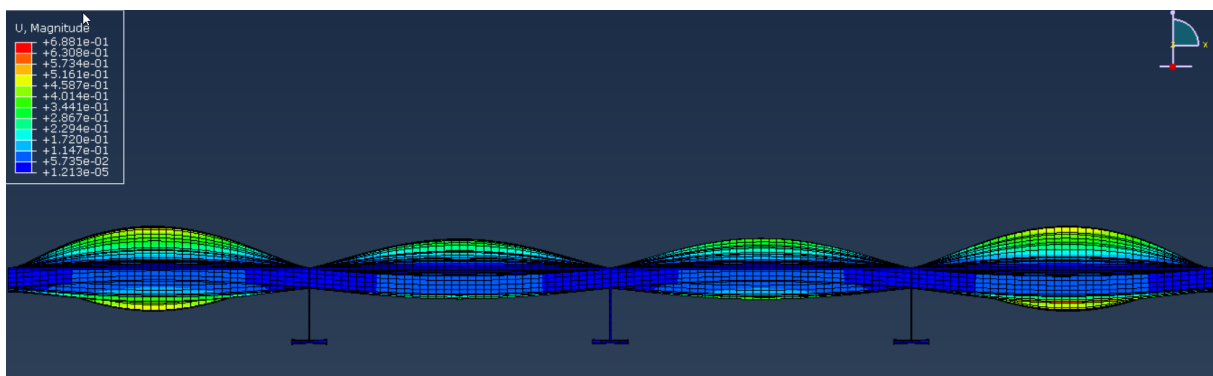
Figure 23-Local imperfection pattern 1



(a) Plate



(b) Stiffener sideview



(c) Girder side view

Figure 24-Local imperfection pattern-2

Since every node in the model has its own specific displacement from each eigenmode. The eigenmode nodal displacement of each node will be multiplied by the scale factor to provide the contribution of that eigenmode to the final imperfections in the non-linear analysis.

The relation between the scale factor and the nodal displacement to the nodal final imperfection amplitude is shown

$$\text{Final nodal imperfection} = U_L \times F_L + U_G \times F_G$$

Equation 5-1

where,

Final nodal imperfection: is the final scaled node displacement that will be introduced to the non-linear analysis model from the local and global eigen mode patterns.

U_L : the nodal displacement introduced by the local pattern

U_G : the nodal displacement introduced by the global pattern

F_L : local pattern scale factor

F_G : Global pattern scale factor

The DNV-RP-C208 [3] provides a minimum-mid bow imperfection for the global pattern and mid plate in between stiffeners imperfection. Due to the model geometrical properties, the

nodes of the global and local patterns acquired from the eigenmode have a wide range of nodal displacement.

In order to apply a scale factor that would represent a realistic final imperfections pattern in the non-linear analysis model. A study is done to determine the suitable nodal displacement average from each pattern to help determine the scale factor.

The notation of the panel is as shown in Figure 25, where a number from 1 to 20 is assigned to each stiffener spacing (plate between stiffener span), and a letter A,B,C,D is assigned to the four stiffener spans.

Since the middle of spans 5A, 5C shows the largest displacement value, the average displacement of nodes at those locations is calculated.

The average of nodes at mid-span 11A, 11C represent the lowest displacement. The much lower displacement at spans 20 and 1 are not considered due to their close location to the boundary condition, which results in a very low displacement. The average global pattern displacements are shown in Table 10 and Figure 25.

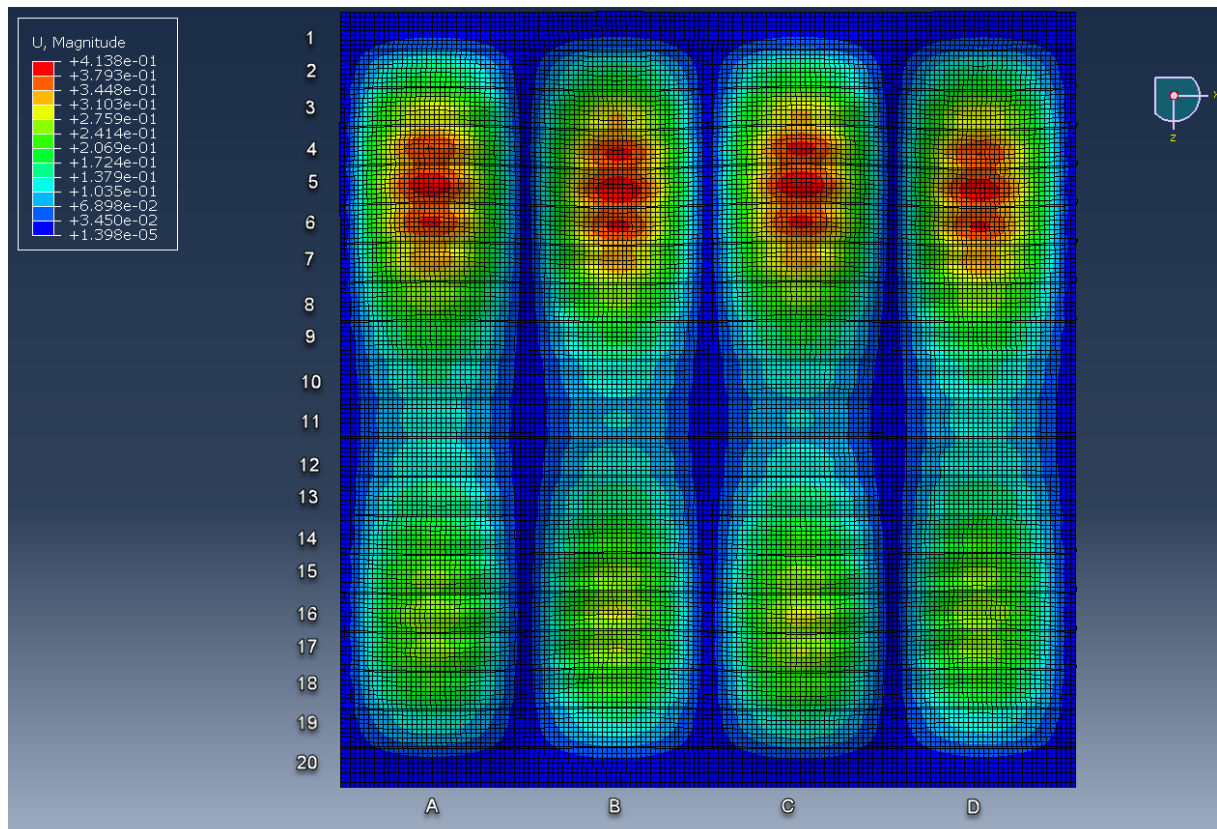


Figure 25- Global imperfection pattern nodal displacement distribution

Table 10-Global Imperfection pattern average displacement

Global imperfection pattern Nodes location	Ug
5A+5C maximum mid-span nodal average displacement	0,380 mm
11A+11C minimum mid-span nodal average displacement	0,1098 mm

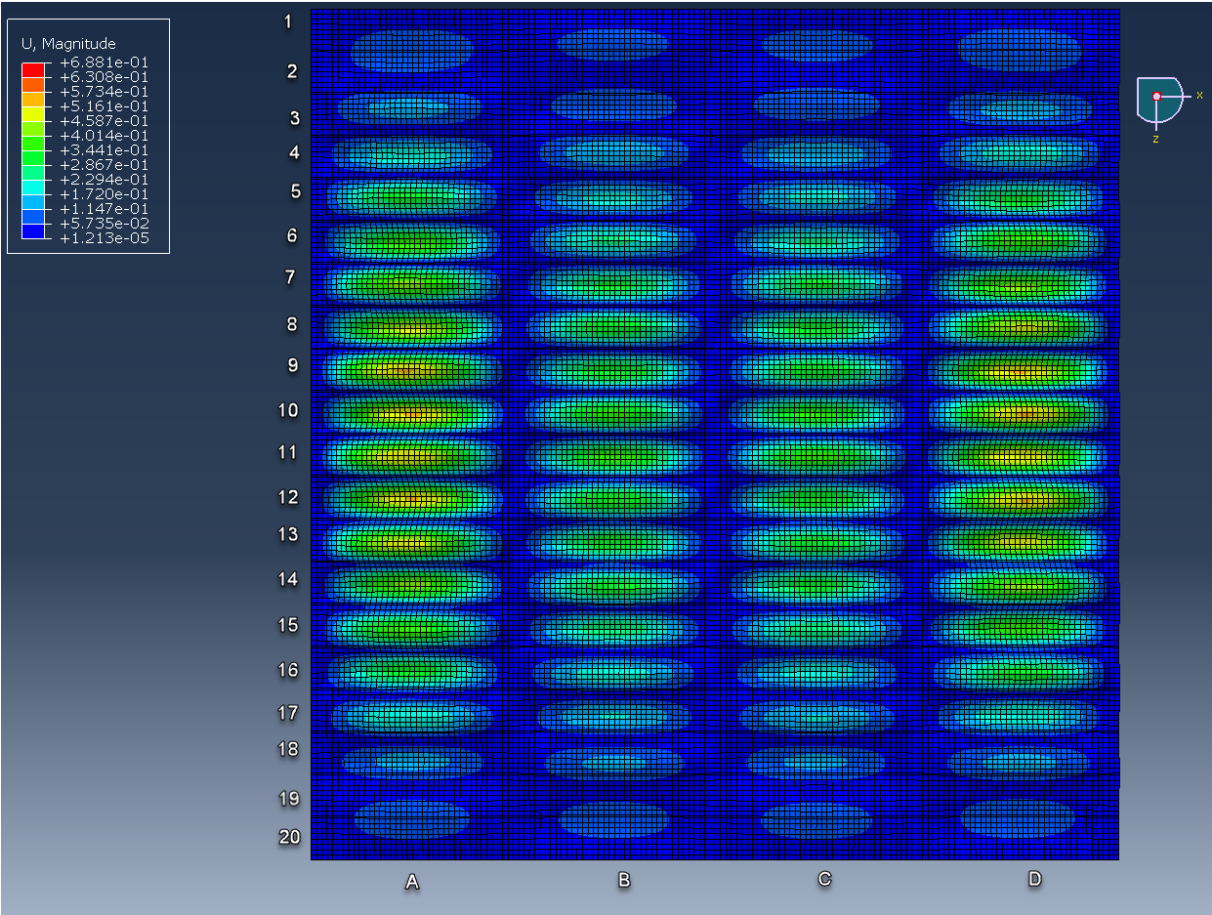


Figure 26-Local imperfection pattern 1 nodal displacement distribution

As shown in Figure 26 and table mid spans 9A and 10D represent the maximum average displacement acquired by this eigenmode, also spans 3A+3C display the lowest displacement average when taking the spans close to the boundary condition out of consideration.

Table 11- local imperfection pattern 1 average displacements

Local imperfection pattern 1 Nodes location	U1
9A+10D Maximum mid-span nodal average displacement	0,410 mm
3A+3C Minimum mid-span nodal average displacement	0,126 mm

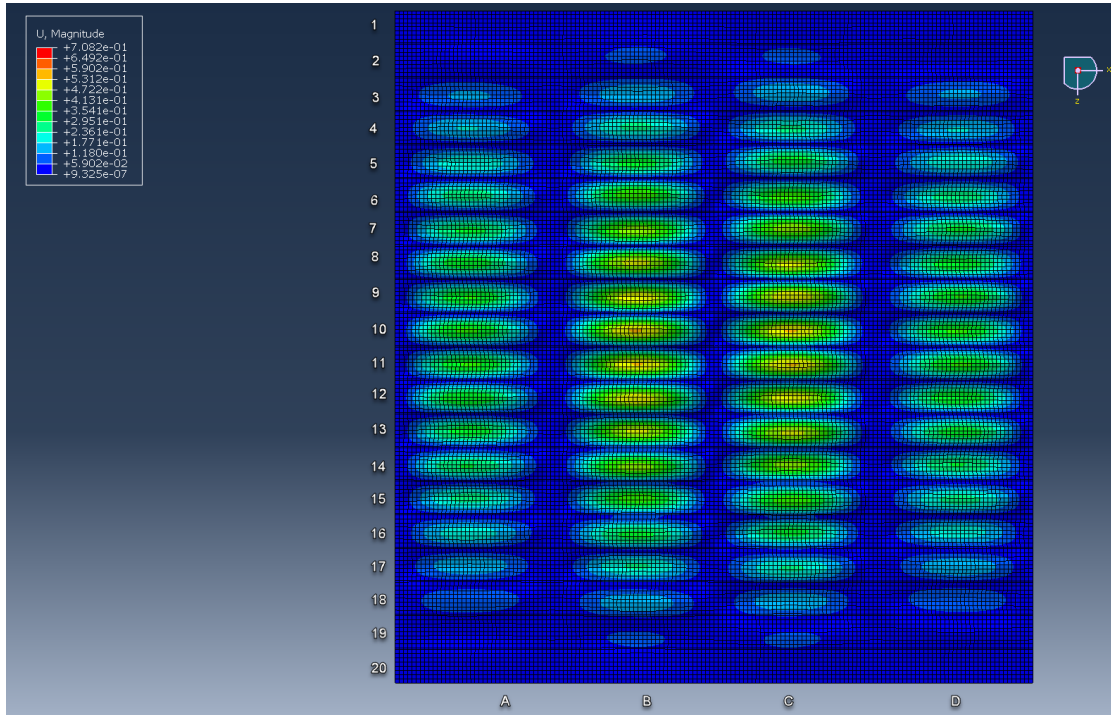


Figure 27--Local imperfection pattern 2 nodal displacement distribution

As shown Figure 27 and table spans 10B and 11C display the highest displacement, and spans 3A displace the lowest average displacement when the spans mostly effected by the boundary are not taken into account.

Table 12- Local imperfection pattern 2 average displacement

Local imperfection pattern 2 Nodes location	UI
10B+11C Maximum mid-span nodal average displacement	0,372mm
3A Minimum mid-span nodal average displacement	0,128 mm

For each case, 3 scale factor trials have been made. 2 additional scale factors are applied to case 1 after consideration of the results discussed in later chapters. The case with scale factor that results in range of imperfection amplitudes within the acceptable range for the investigated panel and results in a buckling capacity close to the benchmark buckling capacity found according to the standards is chosen as a calibrated case for the stiffened panel under compression loads.

Table 13- Applied scale factors

Case	Imperfection Pattern	Uav,max(mm)	Uav,min(mm)	SF1	SF2	SF3	SF4	SF5
1	Global	0,380	0,1098	47.5	63.63	95	85	77.5
	Local 1	0,410	0,126	18.18	18.18	18.18	18.18	18.18
2	Global	0,380	0,1098	8.9	63.63	95	-	-
	Local 2	0,372	0,128	31.67	18.81	18.18	-	-

5.6 Results

For each scale factor, 3 non-linear buckling analysis is performed, only with local imperfection pattern, only on global imperfection pattern, and the combined case. To determine the case with imperfections that gives results of the calibration buckling capacity, the results are represented as force (MN) to displacement (mm) of the nodes in Face 1(Figure 16). The face where the load is applied.

ABAQUS combine the local imperfection pattern and global imperfections pattern on one imperfection pattern to be used in the non-linear analysis. The combined pattern for Case 1 is shown in Figure 28 , for case 2 it is shown in Figure 29. The following graphs will show the results of the analysis done.

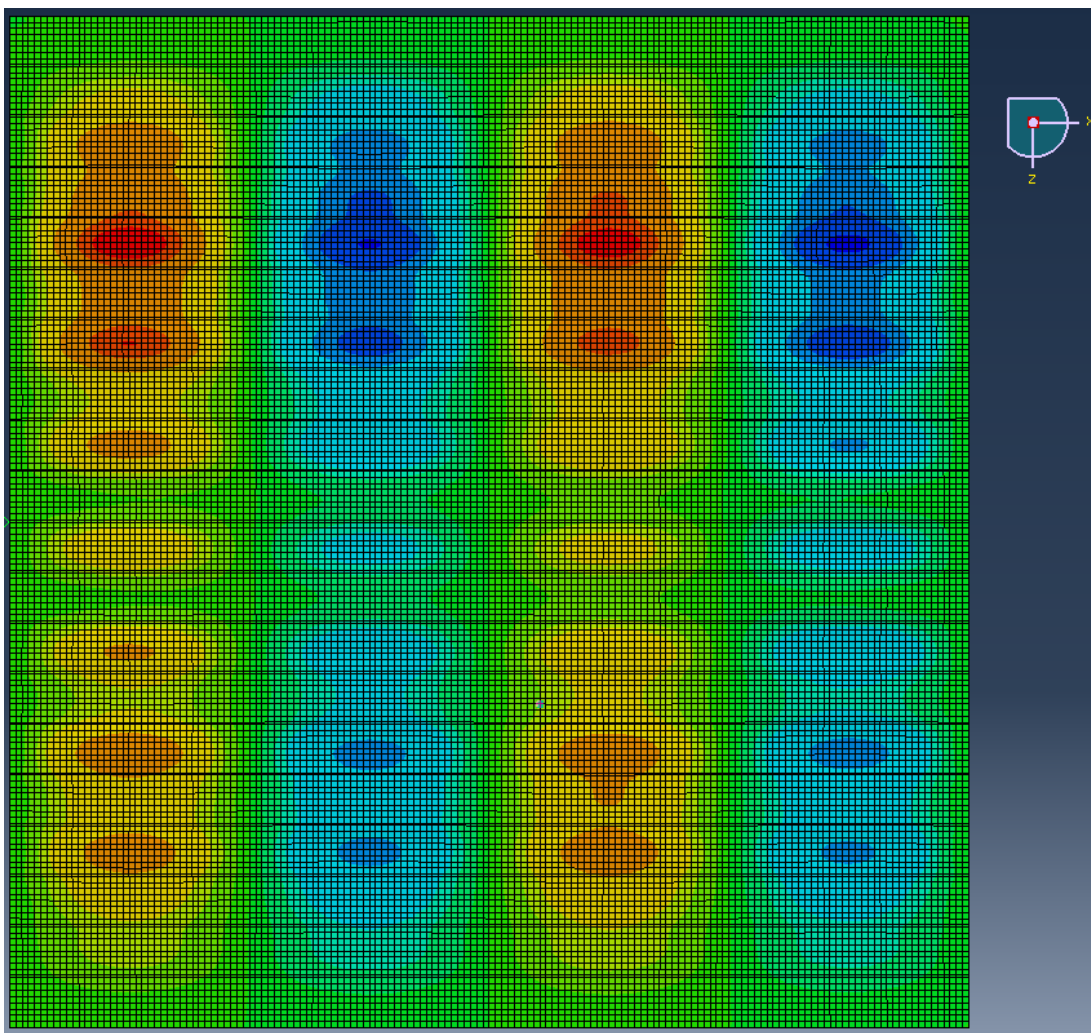


Figure 28-Combined imperfection pattern-Case 1

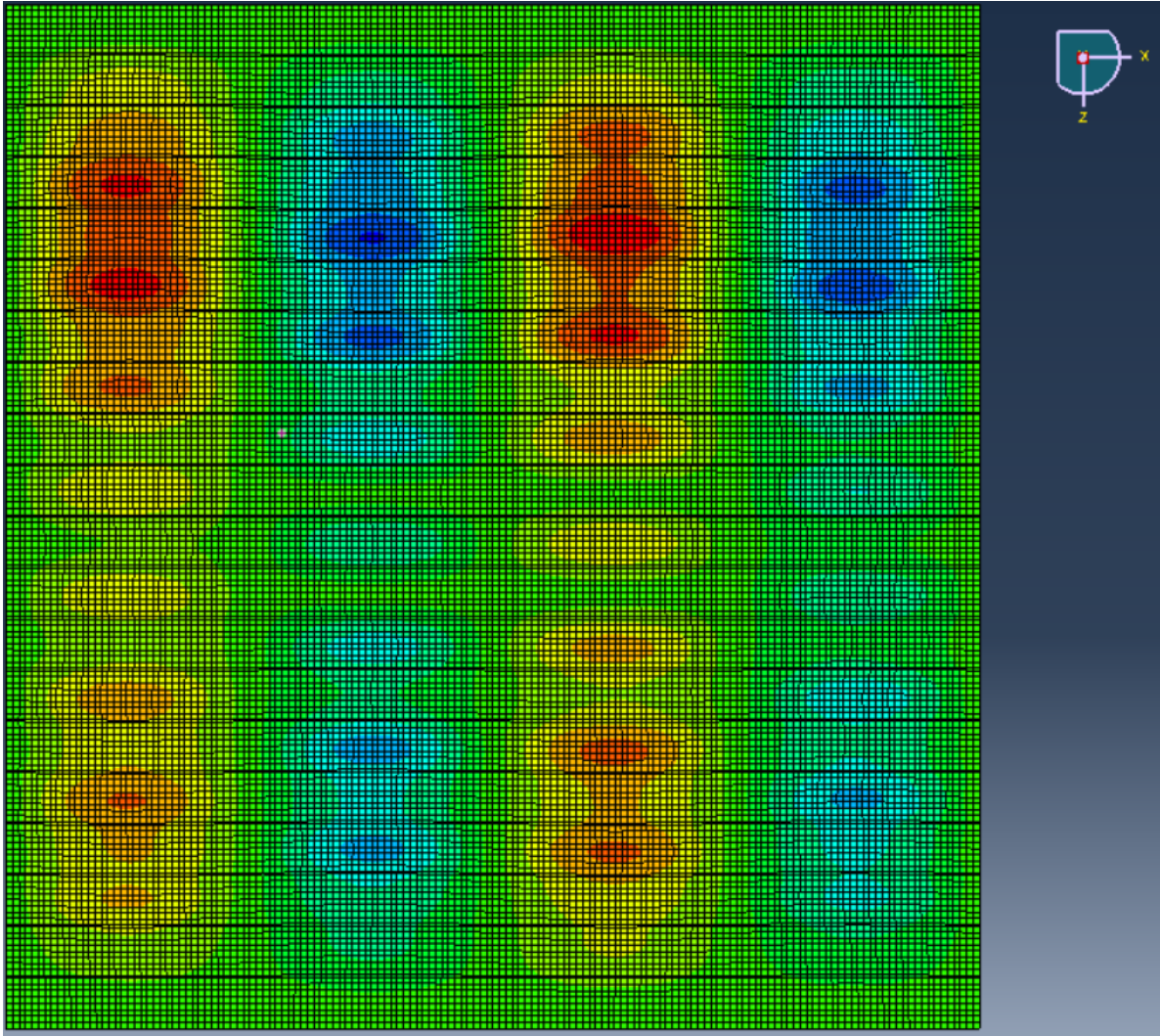


Figure 29- Combined imperfection pattern-Case 2

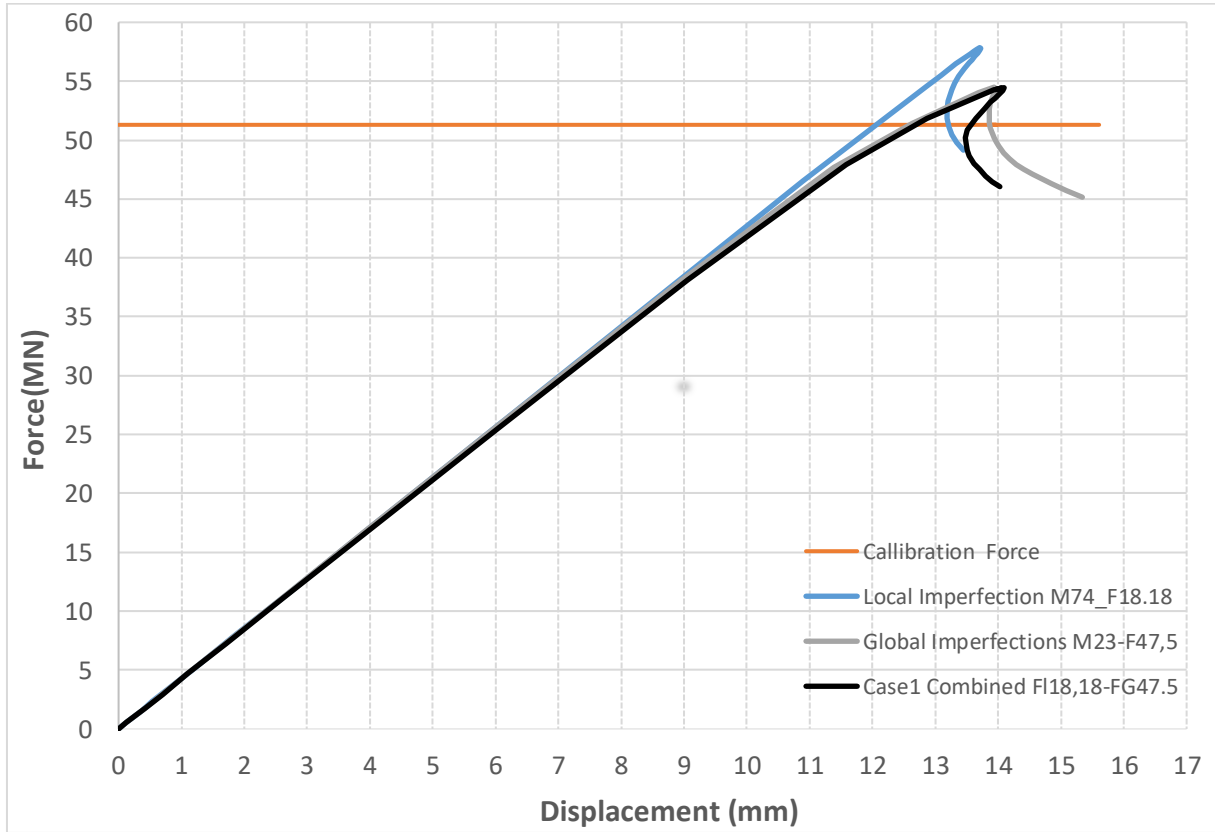


Figure 30- Case 1/SF1 non-linear buckling capacity

Table 14- Case1/SF1 Capacity deviation percentage

Imperfection pattern for Case1-SF1	Capacity deviation %
Local imperfection pattern percentage	11,3%
Global imperfection pattern percentage	5,9%
Combined percentage	5,7%

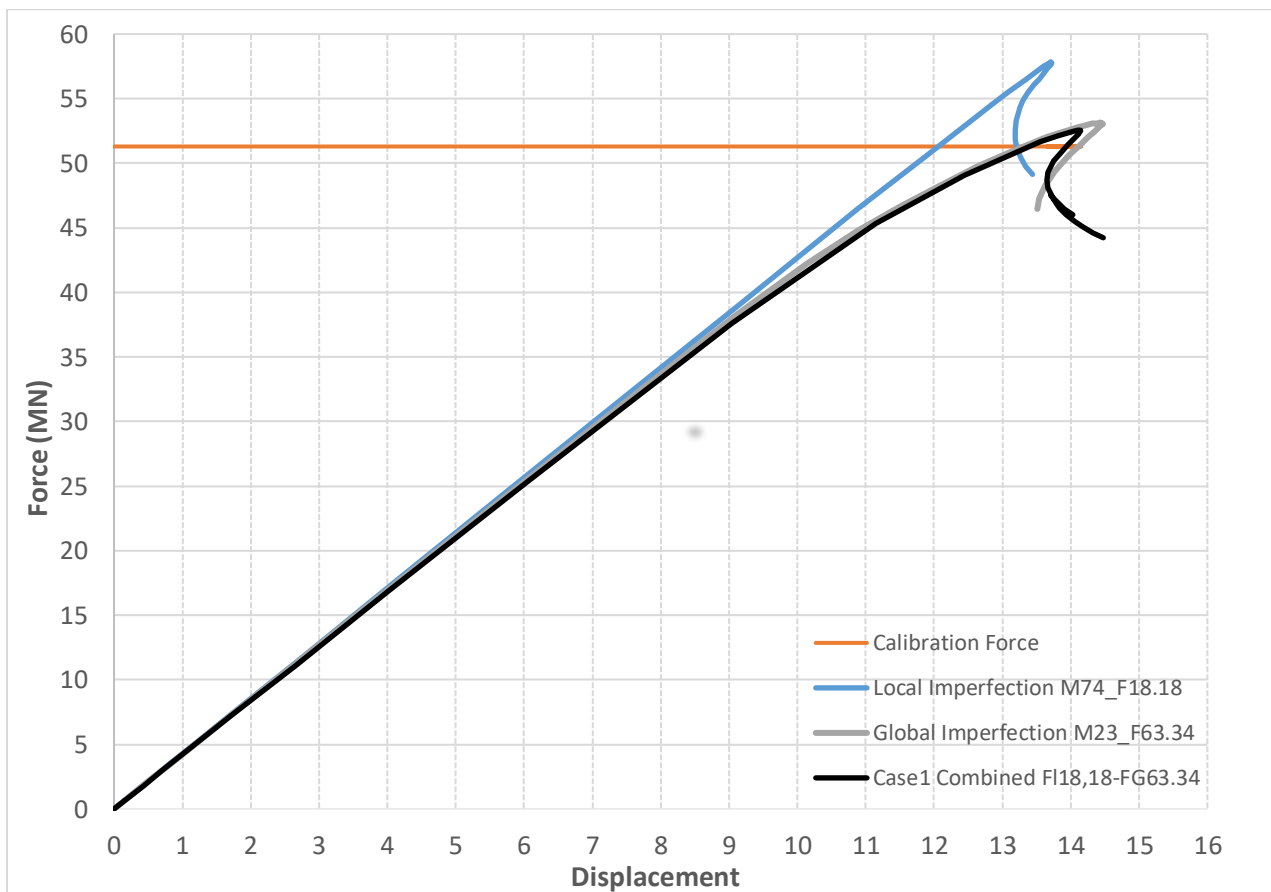


Figure 31-Case 1/SF2 non-linear buckling capacity

Table 15-Case1/SF2 Capacity deviation percentage

Imperfection pattern for Case1-SF2	Capacity deviation %
Local imperfection pattern percentage	11,32%
Global imperfection pattern percentage	3,6%
Combined percentage	2,3%

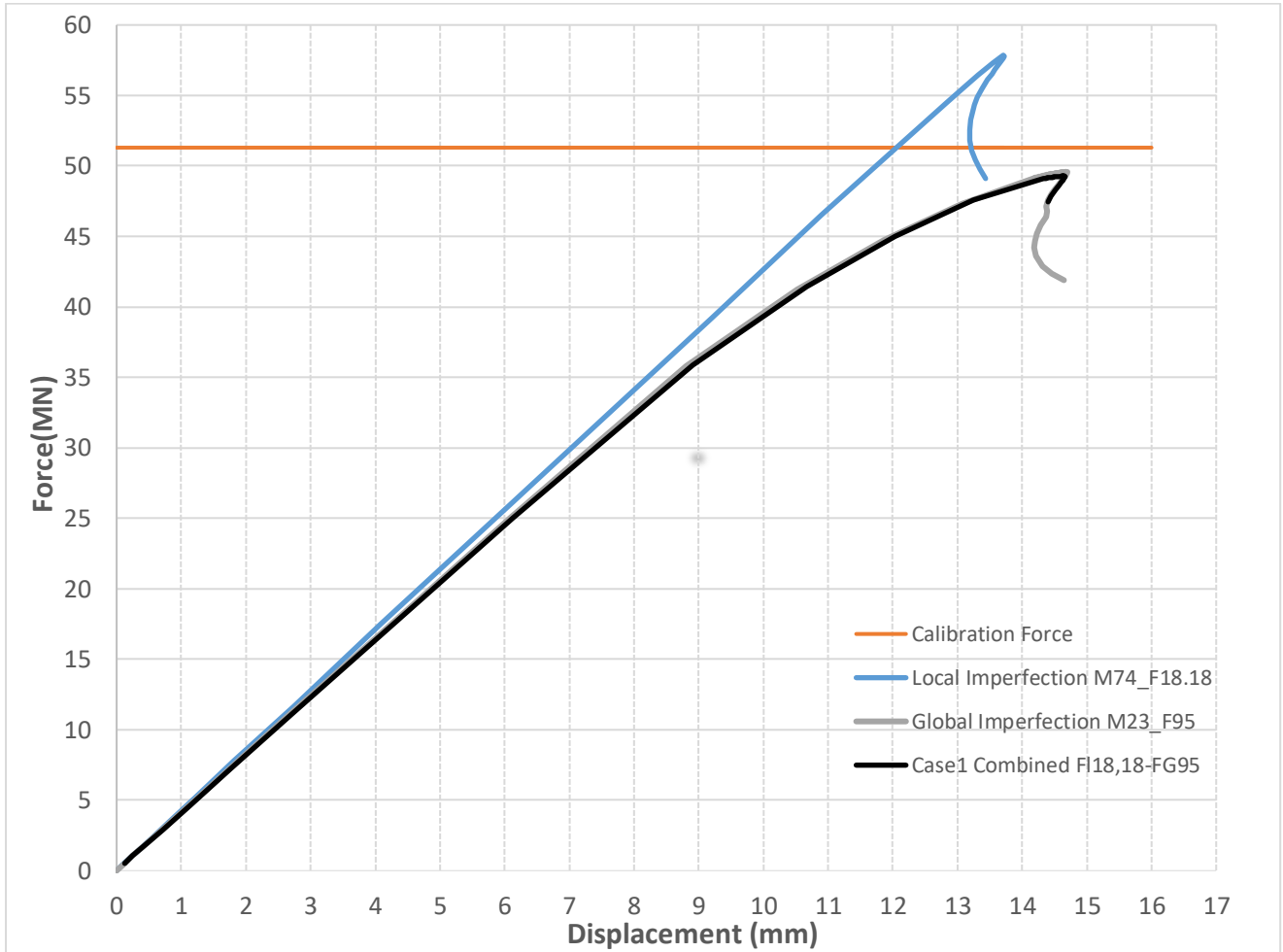


Figure 32-Case 1/SF3 non-linear buckling capacity

Table 16-Case1/SF3 Capacity deviation percentage

Imperfection pattern for Case1-SF2	Capacity deviation %
Local imperfection pattern	11,33%
Global imperfection pattern	-3,46%
Combined Pattern	-4,10%

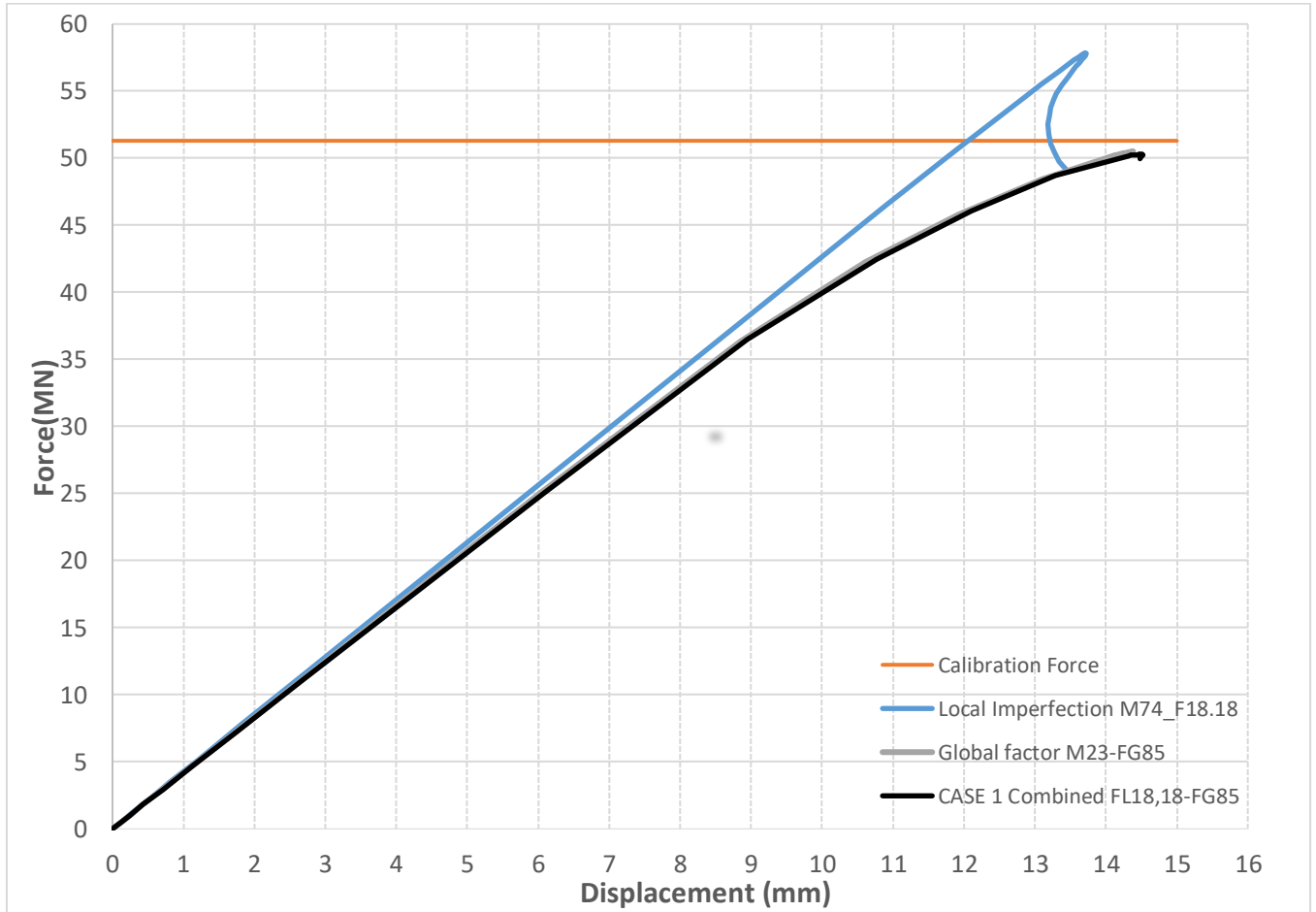


Figure 33-Case 1/SF4 non-linear buckling capacity

Table 17-Case1/SF4 Capacity deviation percentage

Imperfection pattern for Case1-SF2	Capacity deviation %
Local imperfection pattern	11,33
Global imperfection pattern	-1,15
Combined Pattern	-2,03

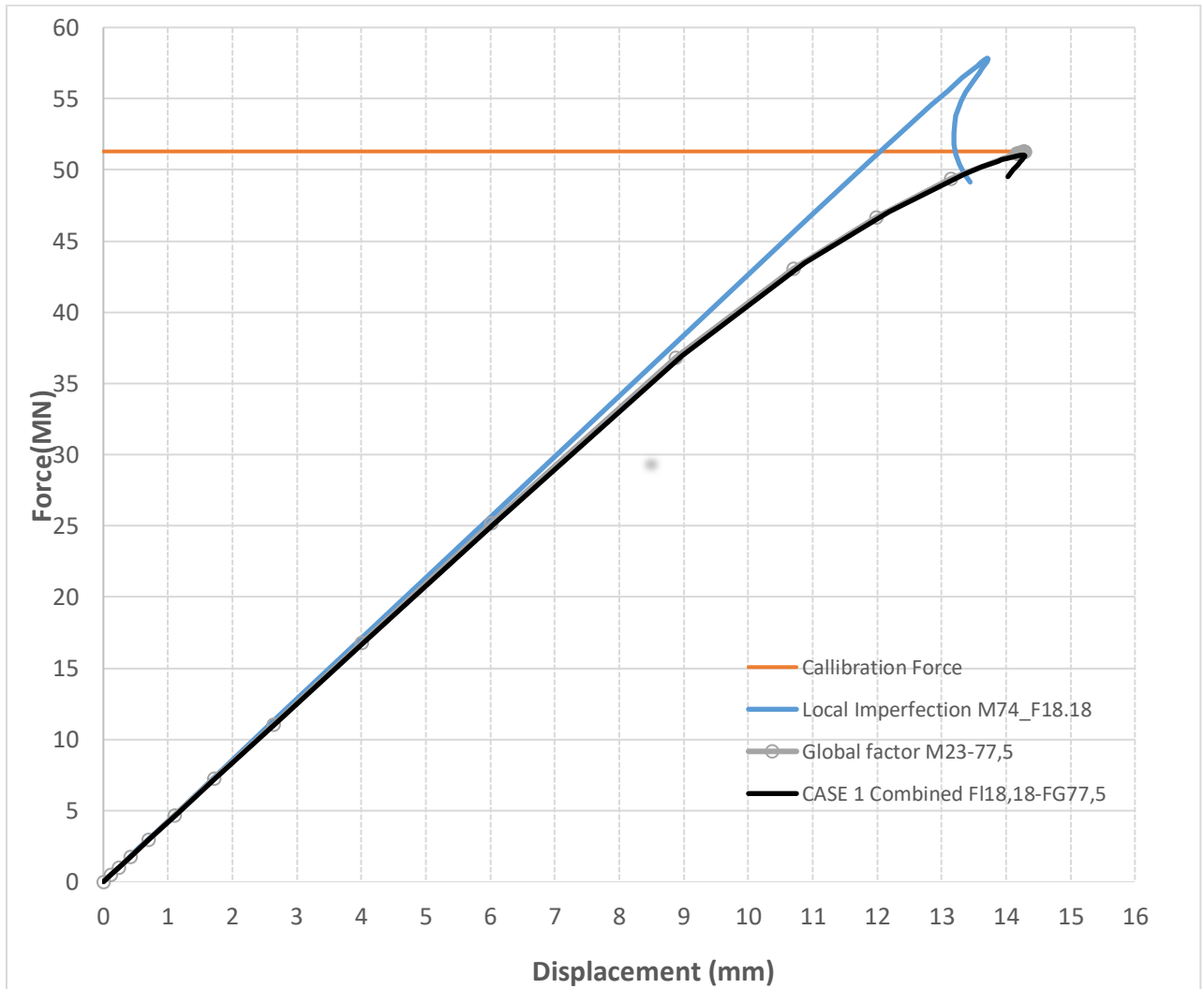


Figure 34-Case 1/SF5 non-linear buckling capacity

Table 18-Case1/SF5 Capacity deviation percentage

Imperfection pattern for Case1-SF2	Capacity deviation %
Local imperfection pattern	11,33
Global imperfection pattern	-0,01
Combined Pattern	-0,51

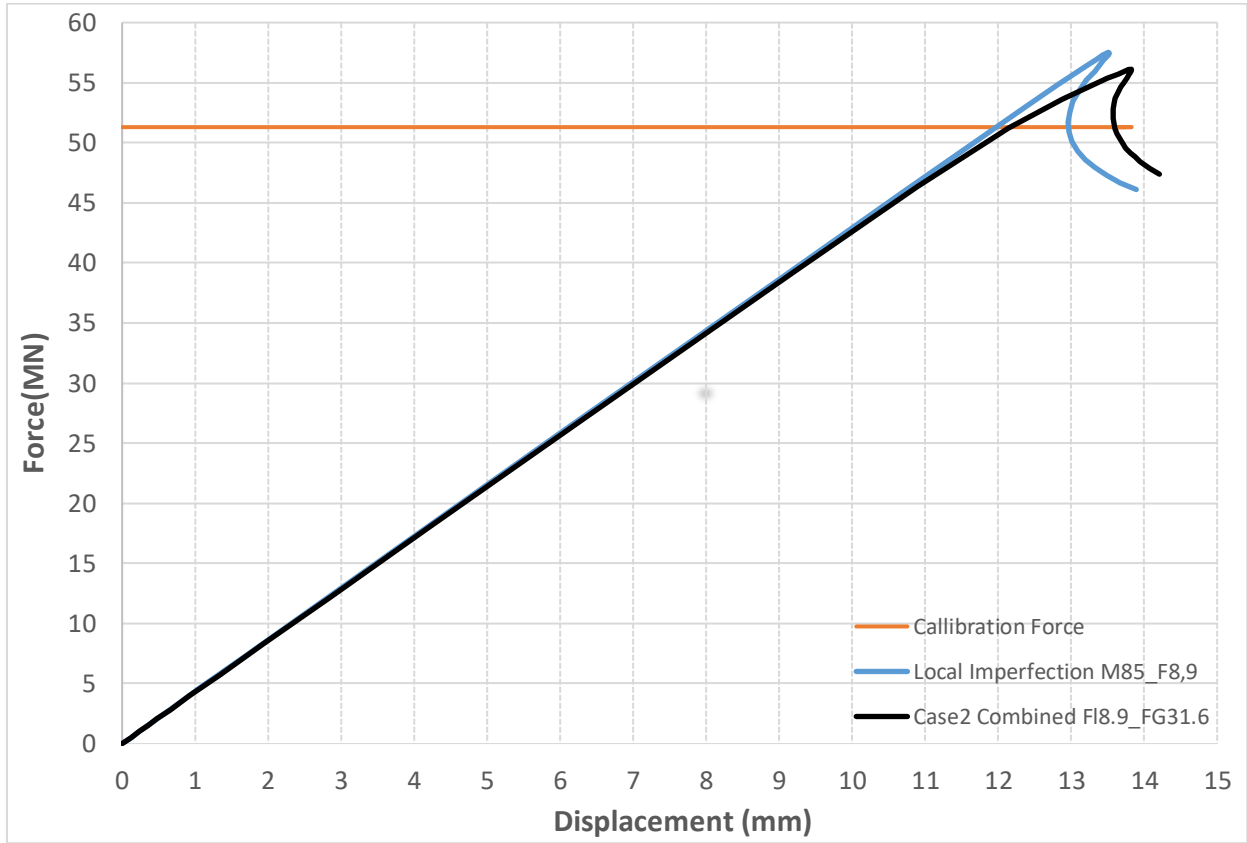


Figure 35-Case 2/SF1 non-linear buckling capacity

Table 19-Case2/SF1 Capacity deviation percentage

Imperfection pattern for Case1-SF2	Capacity deviation %
Local imperfection pattern	10,82%
Combined Pattern	8,6%

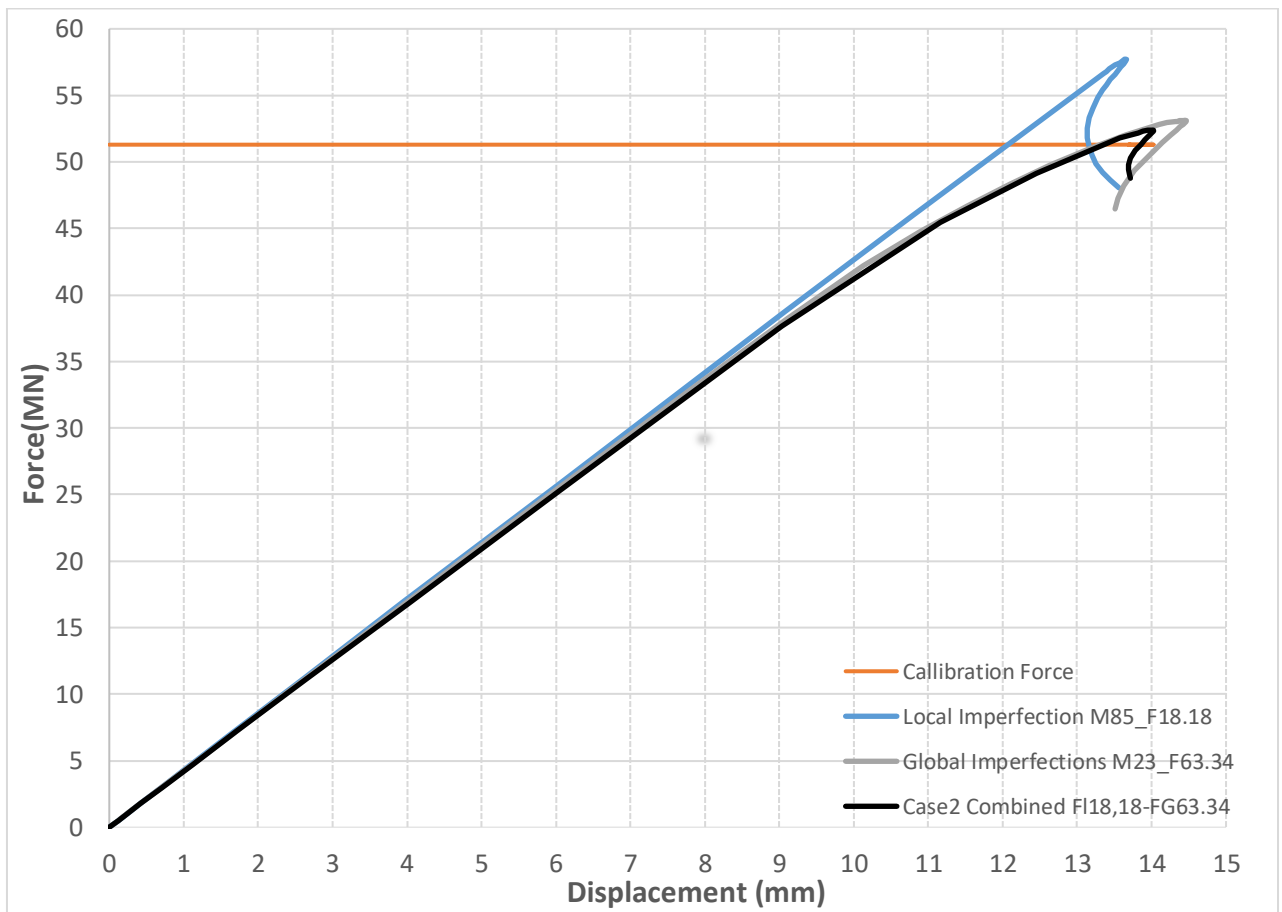


Figure 36--Case 2/SF2 non-linear buckling capacity

Table 20-Case2/SF2 Capacity deviation percentage

Imperfection pattern for Case1-SF2	Capacity deviation %
Local imperfection pattern	11,11%
Global imperfection pattern	3,45%
Combined Pattern	2,09%

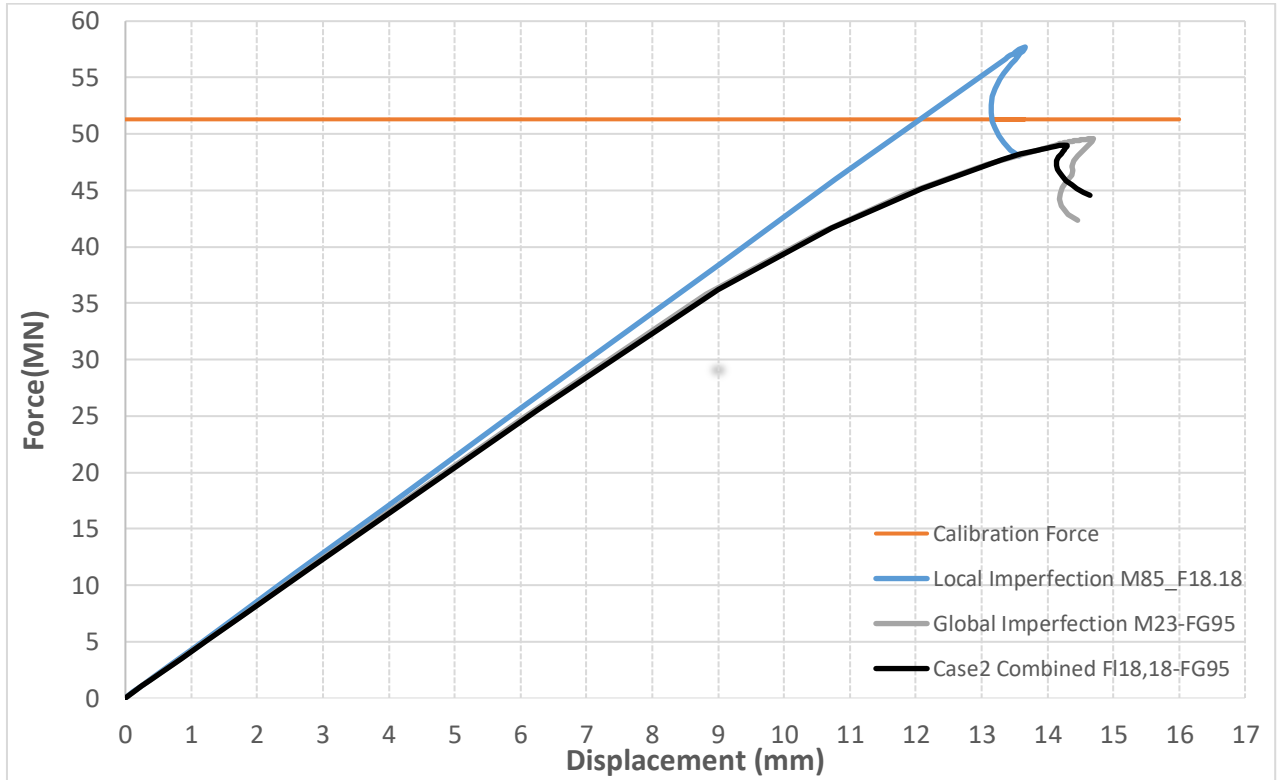


Figure 37--Case 2/SF3 non-linear buckling capacity

Table 21-Case2/SF3 Capacity deviation percentage

Imperfection pattern for Case1-SF3	Capacity deviation %
Local imperfection pattern	11,11%
Global imperfection pattern	-3,46%
Combined Pattern	-4,68%

Chapter- 6 Discussion and Compression of the Results

This chapter discusses the results acquired from the non-linear analysis and clarifies the reasons for choosing the case of the calibration.

6.1 Discussion of results of non-linear analysis

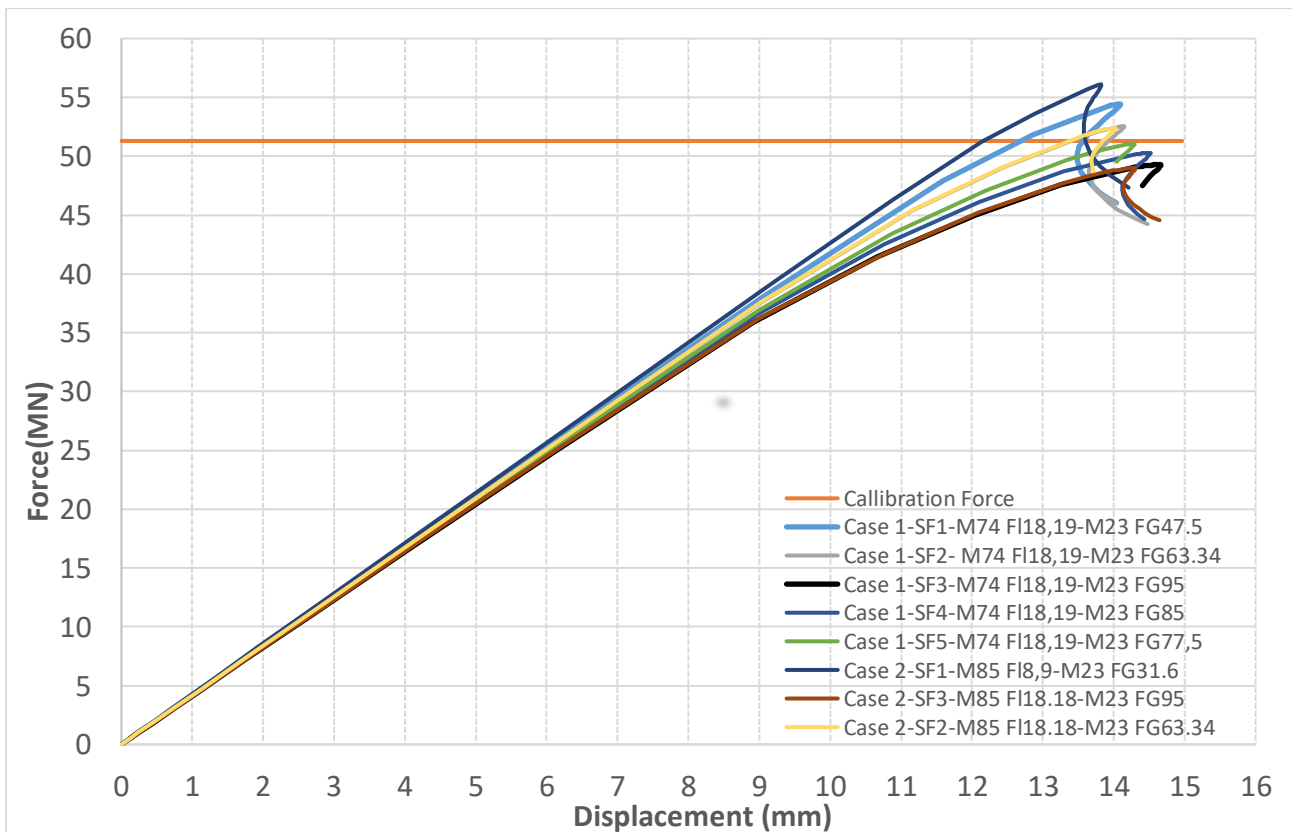


Figure 38- Comparison of the combined patterns cases, nonlinear buckling analysis results

Table 22- Result summary

Case	Imperfection Pattern	Imperfection magnituded of combined imperfection pattern (mm)					Diversioin to Calibration Capacity % (Combined Patterns)				
		SF1	SF2	SF3	SF4	SF5	SF1	SF2	SF3	SF4	SF5
1	Global	5,2-25,6	2,3-31,63	2,29-43,55	2,29-39,75	2,29-36,9	+5,7%	+2,3%	-4,1	-2,30 %	-0,51
	Local 1										
2	Global	4-11,78	2,4-31,17	2,3- 42,86	-	-	+8,9%	+2,09	-4,68%	-	-
	Local 2										

The capacity analysis figures in chapter 5.6 show that since the contribution of imperfections for the global pattern is larger, the buckling capacities are determined using only the global imperfection pattern which shows closer results to the calibration load than the local imperfection pattern. The contribution from the global pattern is higher because the span is larger (stiffener span between girders) and equal to 3800 mm, while for local imperfections the span (stiffener spacing) was 800 mm.

In order to choose the best factors with acceptable imperfection displacement range along the panel, an educated guess to start with factor that would result in combined imperfections around double the recommended from DNV-C208. The chosen factors resulted with the ranges 5,2-25,6 mm along the whole panel for case 1 and imperfection range closer to the recommend values in DNV-C208 (4-11,8 mm) while the recommend is 13,5 mm for the combined case. Both these cases resulted in buckling capacities with a 5,7- 8,9% over estimation of the buckling capacities for this panel. This can be explained by the difference in the pattern shape since the local and global imperfection patterns recommended by DNV-C208 assumes an equal imperfection magnitude along the whole panel. The eigen mode analysis of this panel and due to the panel geometrical properties did not provide global or local modes with equal imperfection magnitudes at the mid-spans.

It can be seen in Table 22 that the average imperfection range SF2 and SF3 is very close in case 1 and case 2. This is done to determine the case with the local imperfection pattern that results in a buckling capacity closer and under the calibration capacity. Table 22 and Figure 38 show that in a higher imperfection magnitude, local pattern 1 in case 1 provide a capacity 0,58% closer to the calibration capacity than local pattern 2. This is taking into account that the global pattern imperfection contribution is the same for both cases. For this reason, case 1 is chosen to continue with the calibration process with SF4 and SF5.

As demonstrated by Figure 38, SF3, SF4 ,SF5 for case 1 and SF3 for case 2 provides estimates of buckling capacity lower than the calibration capacity. However, SF3 for case 2 and case 1 provide an underestimation of the capacity of 4,1% and 4,68% while introducing 15% higher imperfection magnitude than case 1 SF5. Also, case 1-SF4 represents a larger underestimation of the buckling capacity with higher introduced imperfection magnitude than SF5. Since case 1-SF5 provides only an underestimation of 0,5% of the calibration buckling capacity, it is chosen as the calibration case.

6.2 Discussion of calibration case results

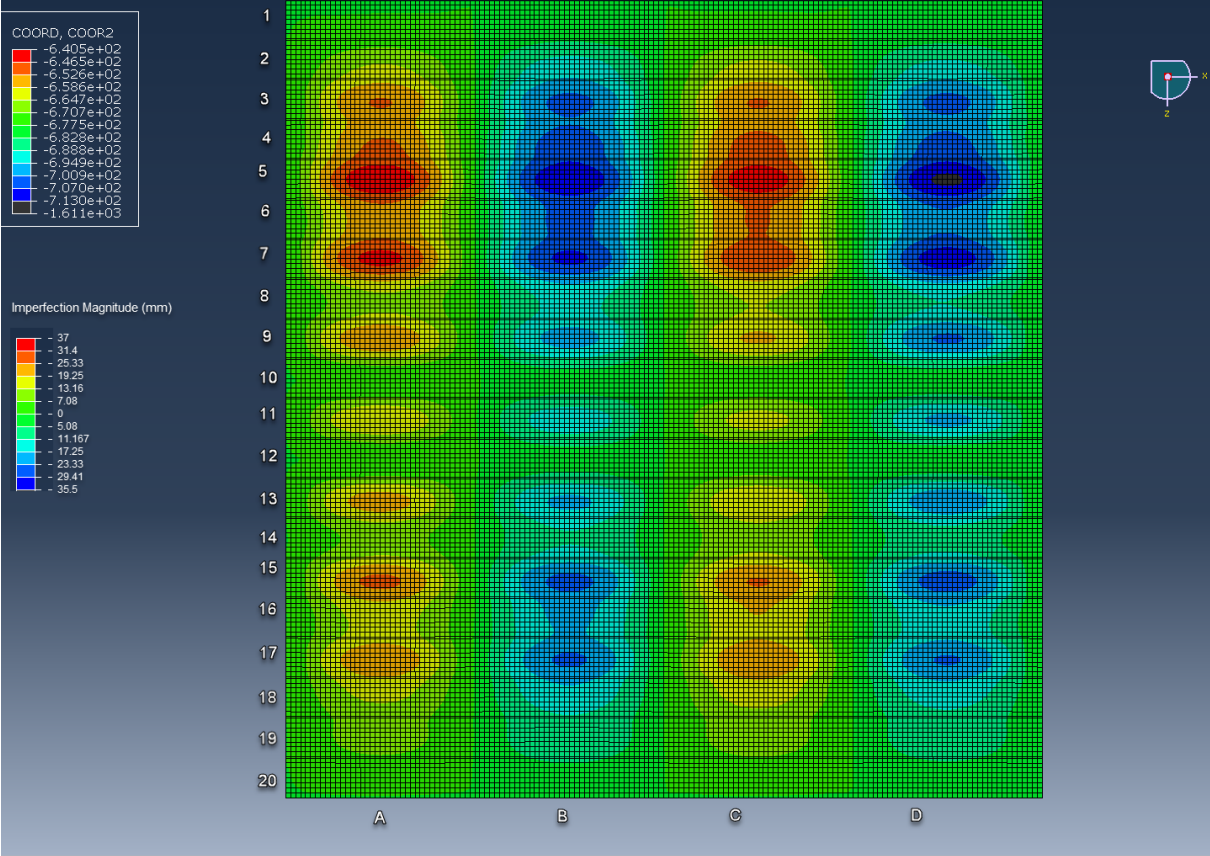


Figure 39- Calibrated case imperfection magnitude and distribution

Figure 39 demonstrates the imperfection distribution and magnitude in case1-SF5. The COOR2 output is the coordination of each node at the Y-axis relatively to the origin coordinate system after the imperfection are applied. The displacement magnitude is calculated by subtracting the COORD2 of each node after applying the imperfection to the Y coordinate of all the nodes which is $Y=677,5$.

From table the largest imperfection range (31,4-37) mm is mostly concentrated in the middle of spans 5A,5B,5C,5D. There is a lower concentration of high imperfections at 7A,7B,7C,7D, and 15A,15B,15C,15D. This is because the local and global imperfection patterns intersect with their highest magnitudes at those locations. The highest nodal imperfection of 36.9 mm at middle of the mentioned stiffener spans represents 1% the stiffener span length. This is higher than the (13,5 mm) or 0,355% of the stiffener span length (3800mm) which is the DNV-RP-C208 [3] recommend for the case where the maximum imperfections from both patterns intersect. However, the local and global imperfection patterns used in the DNV-RP- C208 have equal imperfection amplitude along the panel. This was not the case due to the geometrical properties of the panel at hand, and the eigenmode analysis provided local and global imperfection pattern with different imperfection magnitude concentrations along the panel.

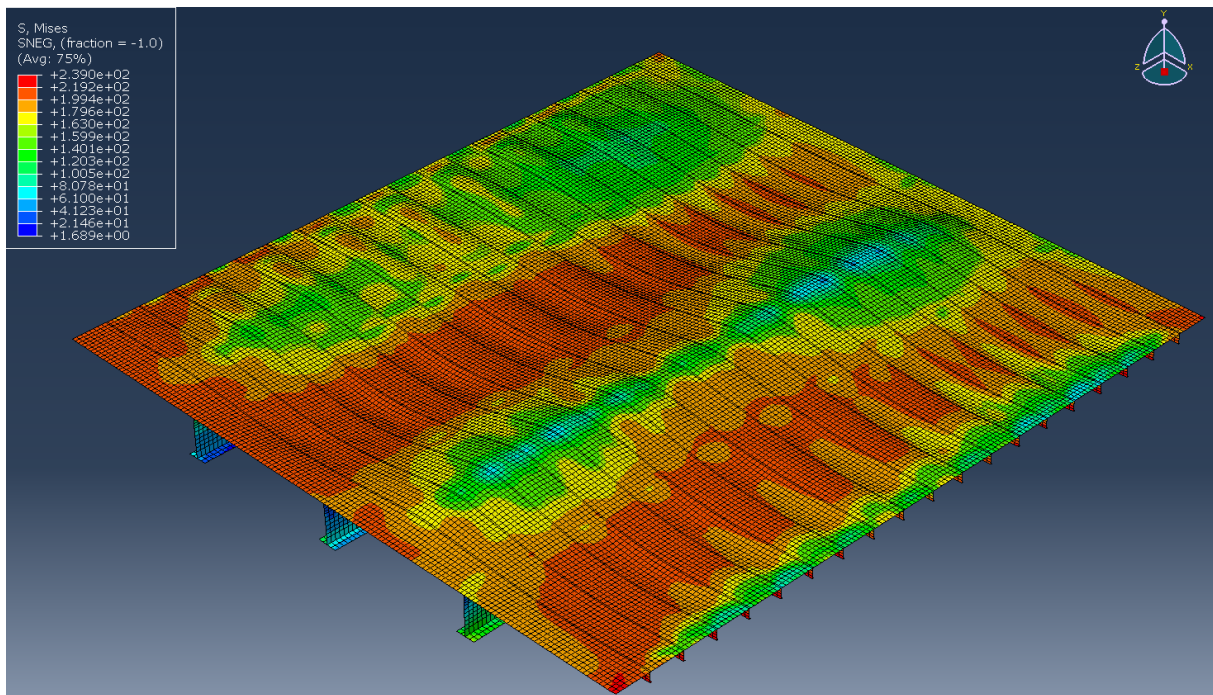


Figure 40- Von-mises stress distribution (MPa)

Figure 40 shows the stress distribution along the panel. The applied load and due to buckling failure do not exceed 99,5% of the applied of the maximum applied load is 169 MPa, this value is exceeded locally along the plate, while the yield stress of 235 MPa is not exceeded in the plate. However, the yield stress it exceeded in the middle of the stiffeners at span C Figure 41 - where the stiffener is under large compression stresses and into the process of buckling. Figure 42 demonstrates that also at the same location the highest maximum principal strain occurs which is 0,5%. The highest strains of 0,5% occur in compression in the panel, so no tensile failure can be expected along the panel. A pressure load of 0,002 MPa was applied on the plate's surface to account for gravity and the deviation to the calibration case decreased to -0,3%.

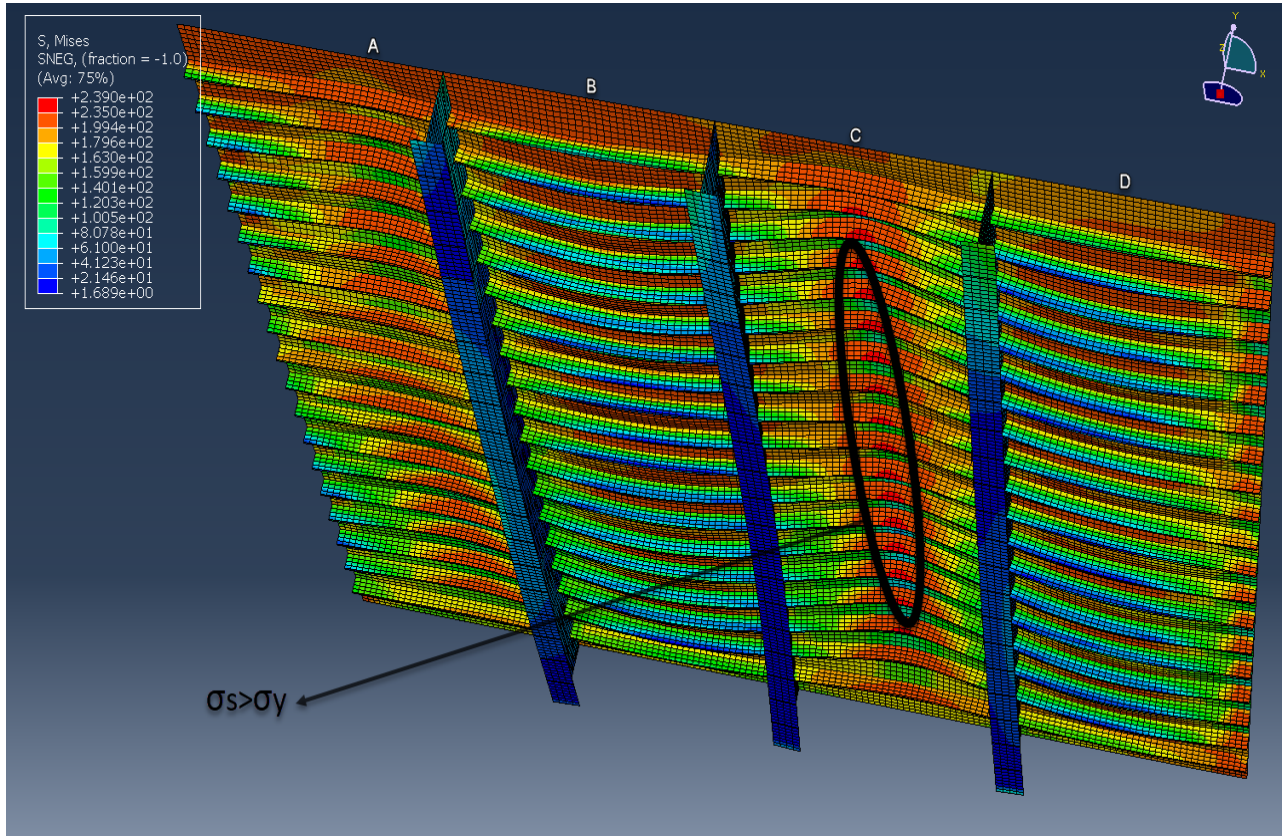


Figure 41- Panel stress concentration

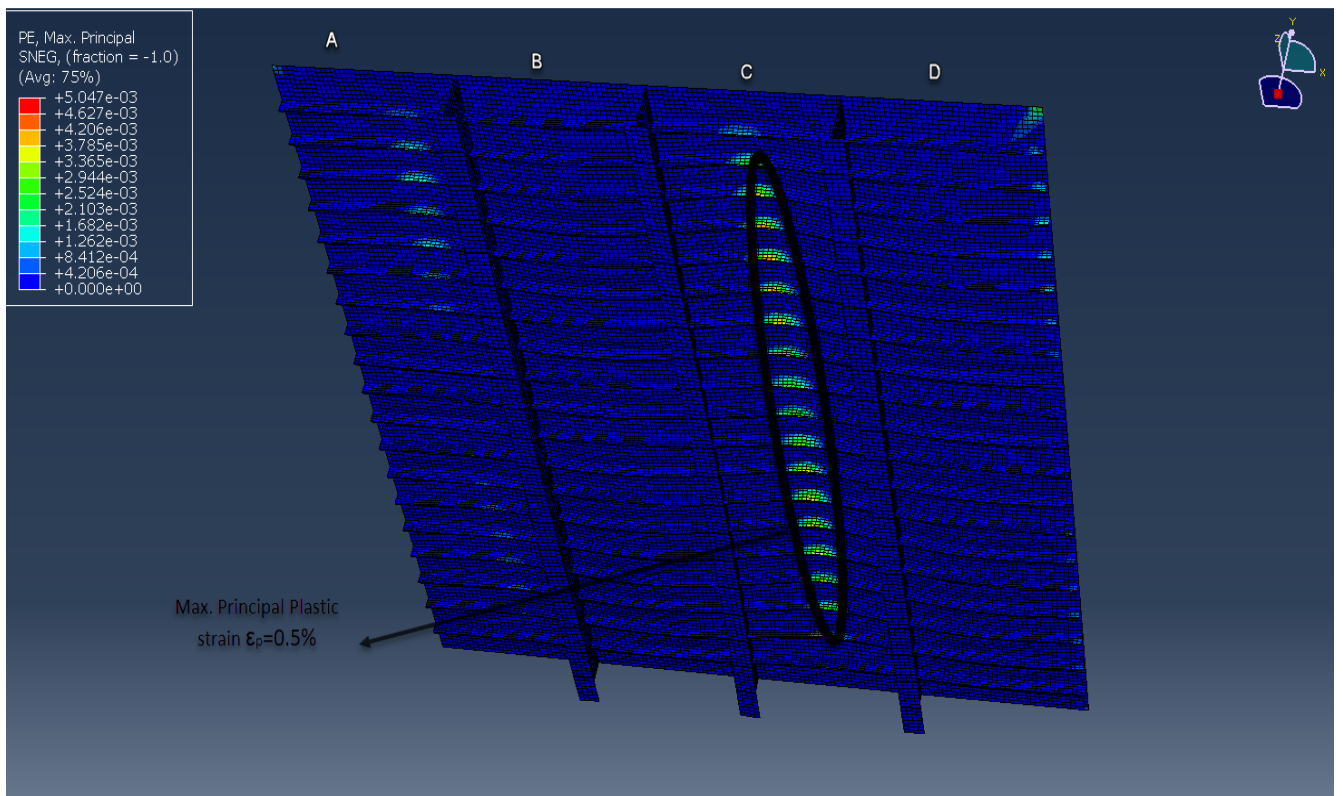


Figure 42- Panel strain concentration

6.3 Effect of holes on buckling capacity of the calibrated model

In order to study the effect of holes on the buckling capacity of the model, the elements of several spans were removed as a first step before the non-linear buckling analysis step starts. The same imperfections patterns and magnitude were applied on the model. Hole 1 shape is shown in Figure 43, Hole 2 is show in Figure 44.

Hole 1 is simulated by removing spans 9B-10B-11B-12B-9C-10C-11C-12C as shown in Figure 43. The area of hole 1 represents 10% of the surface area of the plate, and 20% of the X-direction cross sectional area of span B, and span C. Whereas for Hole 2, spans 6B to 15B are removed from the panel. This equals to 10 plates between stiffener spacing ,50% of the X-direction cross-sectional area of span B, and 12.5% of the surface area.

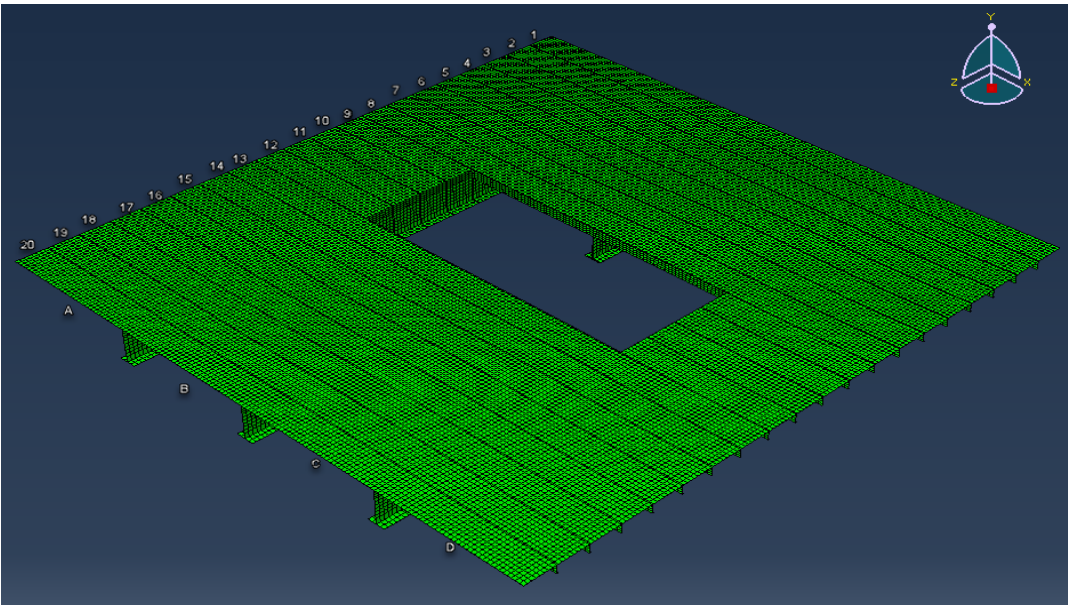


Figure 43- Calibrated model- Hole 1

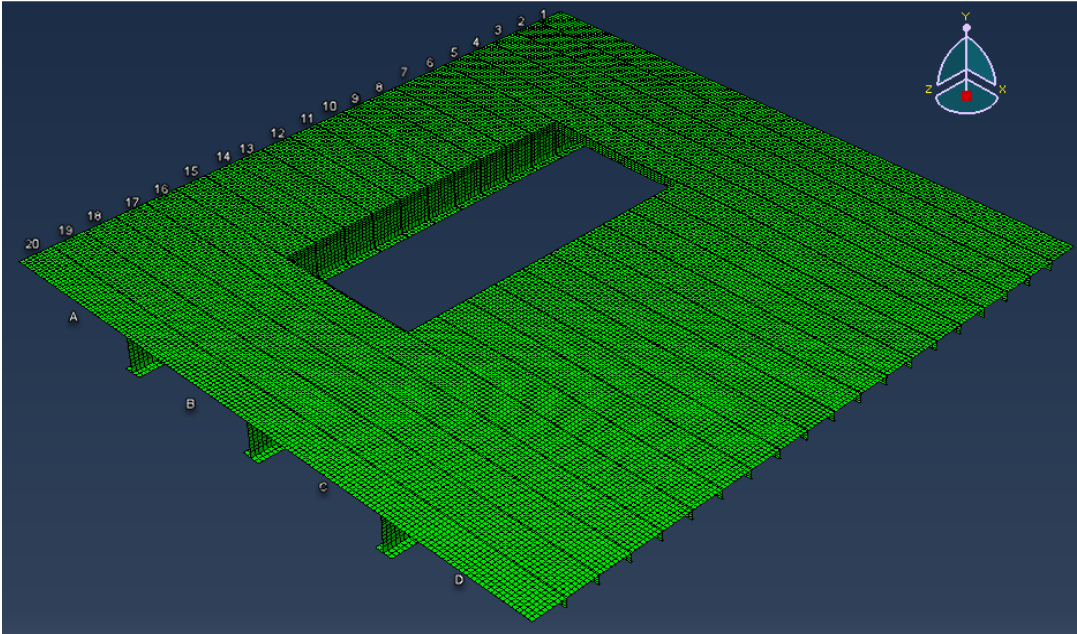


Figure 44- Calibrated model Hole 2

Results of the analysis in Table 23 and Figure 45 show that the reduction percentage of the buckling capacity for the calibrated model for hole 1 is almost equal to the span cross sectional area reduction, even though the area reduction in hole 1 is along spans B and C as shown in Figure 44. The area reduction is connected to the x-direction cross-sectional area reduction of one stiffener span. This is also the case with hole 2 in which the hole is along 10 plates between stiffener spans (stiffener spacing) and one stiffener span (A). The x-direction cross-sectional area reduction was the governing factor where 50% reduction resulted in 47.8% reduction in the buckling capacity of the model, and 20% reduction resulted in 19,6% buckling capacity reduction.

Table 23-Effects of holes on buckling capacity of the calibrated model

	Area reduction		Results	
	Surface	Stiffener span CS	Buckling capacity (MPa)	Reduction of buckling capacity %
Hole 1	10%	20%	137	-19.6%
Hole 2	12.5%	50%	88.7	-47.8%

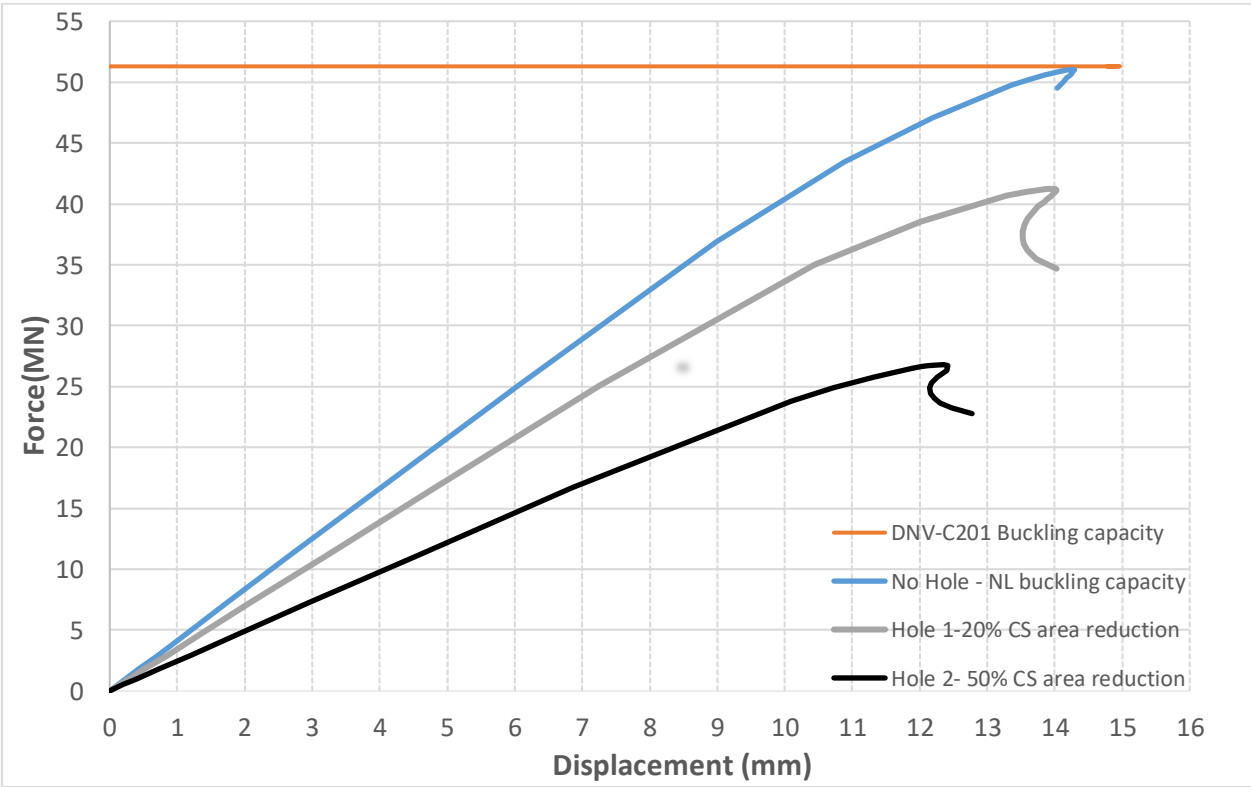


Figure 45- Effect of holes on calibrated model buckling capacity

Chapter- 7 Conclusion and Recommendation for Further Work

7.1 Summary

This thesis includes a literature review on buckling capacity according to DNV-RP-C201[1] standard and DNV-RP-C208 [3] recommended practice. The research context is to apply non-linear finite element method described in DNV-RP-C208 [3] to evaluate the buckling capacity of a ship hull stiffened panel, then compare and calibrate the non-linear buckling capacity to the buckling capacity found by the conventional code DNV-RP-C201[1]. A finite element model was developed using the structural analysis program ABAQUS and introduce geometrical and material nonlinearities into the model. In order to achieve the calibration, the effect of one global and two local imperfection patterns combinations with several imperfection magnitudes were evaluated. After the calibration is achieved, the effects of holes on the buckling capacity of the calibrated non-linear model under uniaxial load and gravity load was investigated.

7.2 Concluding remarks

In order to acquire local and global imperfection patterns several eigen mode analysis are preformed, the patterns chosen to provide the imperfections in the non-linear analysis are the patterns most similar to the those recommended by the DNV-RP-C208. A mid-stiffener span imperfection magnitude that ranged from 0,06% to 1% of the stiffener span length was introduced to the model to achieve 99,7% calibration to the buckling capacity of DNV-RP-C201 standard. The 1% mid-span imperfection magnitude is larger than the DNV recommended 0,355% of the stiffener span length. This is because the patterns acquired for the eigenmode analysis did not provide an equal imperfection magnitude along the mid-spans of the panel as assumed in the DNV-RP-C208 [3] recommended imperfection patterns. This is due to the geometrical properties and boundary conditions of the panel. Also, the assumption of the perfect contact and stress distribution between stiffeners, plates and girders contributes to the larger imperfection introduced to achieve calibration.

Using the calibrated non-linear model, the effect of holes on the buckling capacity under uniaxial load and gravity load was evaluated. The results showed the non-linear buckling capacity reduction of the model correlated with the stiffeners and plate x-direction cross-sectional area reduction that result from the hole in the plate.

7.3 Recommendation for further work

Suggested further work on the calibrated model include,

- 1- Parametric study of the non-linear model, by evaluating the effect of different thicknesses on the buckling capacity of the model. The thicknesses are easily changed because the model is shell element, the imperfection pattern and magnitude are not affected by the change of thickness in the plate, stiffener, or girder.
Then, a calibration capacity according to DNV-RP-C201[1] can be found and a non-linear buckling capacity analysis of the model after changing the thickness can investigate the thickness effect on the buckling capacity of the non-linear model. It can also investigate whether the model imperfection magnitude is still calibrated to the standards when the thickness is changed.
- 2- Since the eigenmode analysis is influenced by mesh size, an approach can be developed where several mesh sizes are investigated under the same conditions and imperfection magnitude to determine the effect of the mesh size on the buckling capacity of the non-linear model.
- 3- The effect of several holes of different sizes and locations on the buckling capacity of the model can be further investigated.
- 4- Calibration of the model to traditional standards after applying different load cases such as transverse and shear loads.

References

- [1] DNV Recommended Practice, *BUCKLING STRENGTH OF PLATED STRUCTURES*, DNV-RP-C201 dated October 2010.

- [2] NORSOK standard, *NORSOK standard N-004, "Design of steel structures,"* 3rd ed. 2013.

- [3] DNV Recommended Practice, *Determination of structural capacity by non-linear finite element analysis methods*, DNV-RP-C208, Amended September 2021.

- [4] T. Putranto, M. Kõrgesaar, J. Jelovica, K. Tabri, and H. Naar, "Ultimate strength assessment of stiffened panel under uni-axial compression with non-linear equivalent single layer approach," *Mar. Struct.*, vol. 78, p. 103004, Jul. 2021, doi: 10.1016/j.marstruc.2021.103004.

- [5] O. Ozguc, "Assessment of Buckling Behaviour on an FPSO Deck Panel," *Pol. Marit. Res.*, vol. 27, pp. 50–58, Sep. 2020, doi: 10.2478/pomr-2020-0046.

- [6] J. K. Paik and A. K. Thayamballi, *Ultimate limit state design of steel plated structures*. Chichester, England ; Hoboken, NJ: J. Wiley, 2003.

- [7] R. D. Cook, D. S. Malkus, and M. E. Plesha, *Concepts and applications of finite element analysis*, 4th ed. New York: Wiley, 1989.

- [8] Cho, Sang-Rai & Kim, Hyun-Su & Doh, Hyung-Min & Chon, Young-Kee. "Ultimate strength formulation for stiffened plates subjected to combined axial compression, transverse compression, shear force and lateral pressure loadings". *Ships and Offshore Structures*. 8. 10.1080/17445302.2013.810492., 2013.

- [9] Ozguc O, Das PK, Barltrop N. 2007. "The new simple design equations for the ultimate compressive strength of imperfect stiffened plates", *Ocean Eng.* 34:970–986.

- [10] Shengming Zhang "A review and study on ultimate strength of steel plates and stiffened panels in axial compression, *Ships and Offshore Structures*", 11:1, 81-91.

- [11] DNV.GL OFFSHORE STANDARDS, *Design of offshore steel structures, general-LRFD method*, DNVGL-OS-C101 Edition July 2018.

- [12] DNVGL-PS, *Stipla, Theory Manual*.

- [13] DNV OFFSHORE STANDARDS, *Fabrication and testing of offshore structures*, DNVGL-OS-C401, Edition July 2020.

[14] Smith, Michael. / ABAQUS/Standard User's Manual, Version 6.9. Providence, RI: Dassault Systèmes Simulia Corp, 2009.

Appendix

Plate-Stiffener buckling check using STIPLA

The screenshot displays the STIPLA software interface for a plate-stiffener buckling check. The window title is "DNVGL-PS: C:\Program Files (x86)\StruProg 2020\STIPLA DNVGL\t=15mm.drps".

General Input:

- Project name: [Empty]
- Project: [Empty]
- Identification: [Empty]
- Test: [Empty]
- Safety format:
 - LRFD Material Factor, gm = 1,00
 - WSD Allowable Usage Factor, UF = 1,00
- Material (MPa):
 - Plate: VL / DNVGL-OS-B101 fyp = 235
 - Stiffener: VL / DNVGL-OS-B101 fys = 235
 - Young's modulus E: 2,10E+5
- Continuous stiffener | Sniped stiffener |
 - Use recommended values for moment factor and buckling length: Yes No
 - Buckling length: Lk = 3758 mm
 - Moment factor - Support: km1 = 12,0
 - Field: km2 = 24,0
 - Recommended values: 1123 km1 = 12 km2 = 24

Geometry & Stresses:

- Geometry (mm):
 - Stiffener span: L = 3800
 - Length of girder: Lg = 16000
 - Plate thickness: t = 15,0
 - Stiff spacing: s1 = 800, s2 = 800
 - Lat tors buck length: Lt = 3800
 - Stiffener profile: BF 240x10,0
- Stresses (MPa):
 - SigxA = -170,0 SigxB = -170,0
 - SigyA = 0,0 SigyC = 0,0
 - Tau = 0,0 psd = 0,002 +/-

Figure: A schematic diagram of the plate-stiffener assembly. It shows a rectangular plate (PL1) supported by a stiffener (PL2). The stiffener is divided into three segments (1, 2, 3) with spacing s1 and s2. The total length is Lt. The diagram also shows the coordinate system (x, y, z) and the applied stresses (Sigx, psd).

Buckling/Section Scantling:

- Buckling Incl. deformation
- Yield Buckling + Yield
- Buttons: More Results, Plate Curve, Stiff Curve, Plate/Stiff Curve, Diagram of Usage Factors
- Optimize z*:

Result:

Control	Interaction Ra...	Reference
STIFFENER BUCKLING CHECK (DNV-RP-C201): (1 = Support, 2 = field; s = stiffener, p = plate)		
se = 653,5 mm Sigxsd = -170,0 MPa Sigysd = 0,0 MPa p0 = 0,000 MPa z* = 2,0 mm		
UF1s = Nsd/Nks1Rd + (M1Sd - NSd*z) / (Ms1Rd * (1 - Nsd/Ne)) + u = 2592,3/2497,6 + (1,9 - 2592,3*0,002) / (87,1*(1 - 2592,3/11367,3)) + 0,000 =	0,99	< 1,00 (Eq 7.50)
UF1p = Nsd/Nkp1Rd - 2*Nsd/N1Rd + (M1Sd - NSd*z) / (Mp1Rd * (1 - Nsd/Ne)) + u = 2592,3/2647,9 - 2*2592,3/3067,1 + (1,9 - 2592,3*0,002) / (471,4*(1 - ...	-0,72	< 1,00 (Eq 7.51)
UF2s = Nsd/Nks2Rd - 2*Nsd/NRd + (M2Sd + NSd*z) / (Ms2Rd * (1 - Nsd/Ne)) + u = 2592,3/2497,6 - 2*2592,3/3067,1 + (1,0 + 2592,3*0,002) / (87,1*(1 - 2...	-0,56	< 1,00 (Eq 7.52)
UF2p = Nsd/Nkp2Rd + (M2Sd + NSd*z) / (Mp2Rd * (1 - Nsd/Ne)) + u = 2592,3/2647,9 + (1,0 + 2592,3*0,002) / (471,4*(1 - 2592,3/11367,3)) + 0,000 =	1,00	< 1,00 (Eq 7.53)
Shear check: Vsd/Vrd = 3,0/286,6 =	0,01	< 0,50 (Ch 7.8)

Figure 46 Plate-Stiffener buckling check using

DNVGL-PS: C:\Program Files (x86)\StruProg 2020\STIPLA DNVGL\t=15mm.drps

File Stiffener profile Print Help

General Input

Project name:

Project:

Identification:

Test:

Safety format

LRFD Material Factor, gm =

WSD Allowable Usage Factor, UF =

Material (MPa)

Plate: VL / DNVGL-OS-B101 fyp=

Stiffener: VL / DNVGL-OS-B101 fys=

Youngs modulus E:

Continuous stiffener | Sniped stiffener

Use recommended values for moment factor and buckling length: Yes No

Buckling length: Lk = mm

Moment factor - Support: km1 Field: km2

Recommended values: 1123 km1 = 12 km2 = 24

Geometry & Stresses

Geometry (mm)

Stiffener span: L =

Length of girder: Lg =

Plate thickness: t =

Stiff spacing: s1 = s2 =

Lat tors buck length: Lt =

Stiffener profile: BF 240x10,0

Stresses (MPa)

SigxA = SigxB =

SigyA = SigyC =

Tau = psd =

Fixation parameter for plate (F300)

Clamped edges (kpp=1.0)

Simply supported edges (kpp=0.5)

Figure

Buckling/Section Scantling

Buckling

Yield

Buckling + Yield

Consider Vsd/Vrd > 0.5

Optimize z?:

More Results

Plate Curve Stiff Curve

Plate/Stiff Curve

Diagram of Usage Factors

Result

Control	Interaction Ra...	Reference
PLATE YIELD CHECK (Points A-D) AND LATERAL CHECK:		
Yield, max in point: A: UF = Sigjd/fyd = 170,0/235,0 =	0,72	< 1,00
Lateral: PL1 - UF = p/pRd = 0,002/0,209 =	0,01	< 1,00
PLATE THICKNESS CHECK (DNVGL-OS-C101, Ch.2 Sec.4 [6.3]):		
Point A: Sigjd = 170,0 MPa UF = tmin/t = 1,94/15,00 =	0,13	< 1,00
STIFFENER YIELD CHECK: (check at points 1-3, plate(p) and stiffener(s)). Effective width se = 800,0		
Point 2p: UF = Sigjd/fyd = 170,4/235,0 =	0,73	< 1,00
Point 1s: UF = Sigx/fyd = 175,1/235,0 =	0,75	< 1,00
STIFFENER SECTION MODULUS CHECK (DNVGL-OS-C101, Ch.2 Sec.4 [6.4]):		
(check at points 1-3, plate(p) and stiffener(s)) Effective width se = 800,0 mm		
Point 1p: Sigjd = 170,0 MPa UF = Zs/Wp = 2,962E+4/2,430E+6 =	0,01	< 1,00
Point 1s: Sigxd = 170,0 MPa UF = Zs/Ws = 2,962E+4/3,744E+5 =	0,08	< 1,00

Figure 47 Plate-stiffener yield and section checks

Results of calculated parameters using STIPA, the number of the equation is reference to the equation number in the standard DNV-RP-C201.

Parameter	Value	unit	Reference	Parameter	Value	unit	Reference
fET	750,041	MPa	Eq 7.31/7.32/7.34	Ch 7.2 Forces			
fT	235,000	MPa	Eq 7.27/7.28	Nsd	2592,330	kN	Eq 7.1
Ch 7.7.3 Resistance				Tauf	0,000		Eq 7.2
Wes	3,708E+5	mm3	Eq 7.68 point 1	Taucrg	16,463	MPa	Eq 7.4
Wep	2,006E+6	mm3	Eq 7.71 point 1	kg	5,566		Eq 7.5
Wes	3,708E+5	mm3	Eq 7.69 point 2	Taucrl	368,227	MPa	Eq 7.6
Wep	2,006E+6	mm3	Eq 7.71 point 2	kl	5,517		Eq 7.7
Ne	11367,340	kN	Eq 7.72	p0	0,000		Eq 7.9/7.10
ie	7,704E+1	mm4	Eq 7.73	c01	0,001		Eq 7.11
lk	3758,019	mm	Eq 7.74	c02	0,001		Eq 7.11
pf	0,091	MPa	Eq 7.75	kc1	38,066		Eq 7.12
				kc2	38,066		Eq 7.12
				lsr	0,000E+0	mm4	Eq 7.12
Parameter	Value	unit	Reference	Parameter	Value	unit	Reference
Ch 7.5.2 Torsional				Ch 7.3 Effective width			
lamdae	0,938		Eq 7.40 plate 1	Cx1	0,817		Plate 1
fep1	176,479	MPa	Eq 7.39 plate 1	Cy1	1,000		Plate 1
n	0,963		Eq 7.38 plate 1	Cx2	0,817		Plate 2
lamdae	0,938		Eq 7.40 plate 2	Cy2	1,000		Plate 2
fep1	176,479	MPa	Eq 7.39 plate 2	se	653,490	mm	
n	0,963		Eq 7.38 plate 2	Ch 7.5 Characteristic			
n	0,963		Eq 7.38 plate 1+2	fe	870,970	MPa	Eq 7.24
C	0,171		Eq 7.36	lamdast	0,519		Eq 7.23
Beta	1,921		Eq 7.35	fks	191,369	MPa	
IT	3800,000	mm		lamdapl	0,519		Eq 7.23
fET	750,041	MPa	Eq 7.31/7.32/7.34	fip	202,886	MPa	
fT	235,000	MPa	Eq 7.27/7.28				

Figure 48- Parameters used in Stiffener plate checks

Girder Buckling check

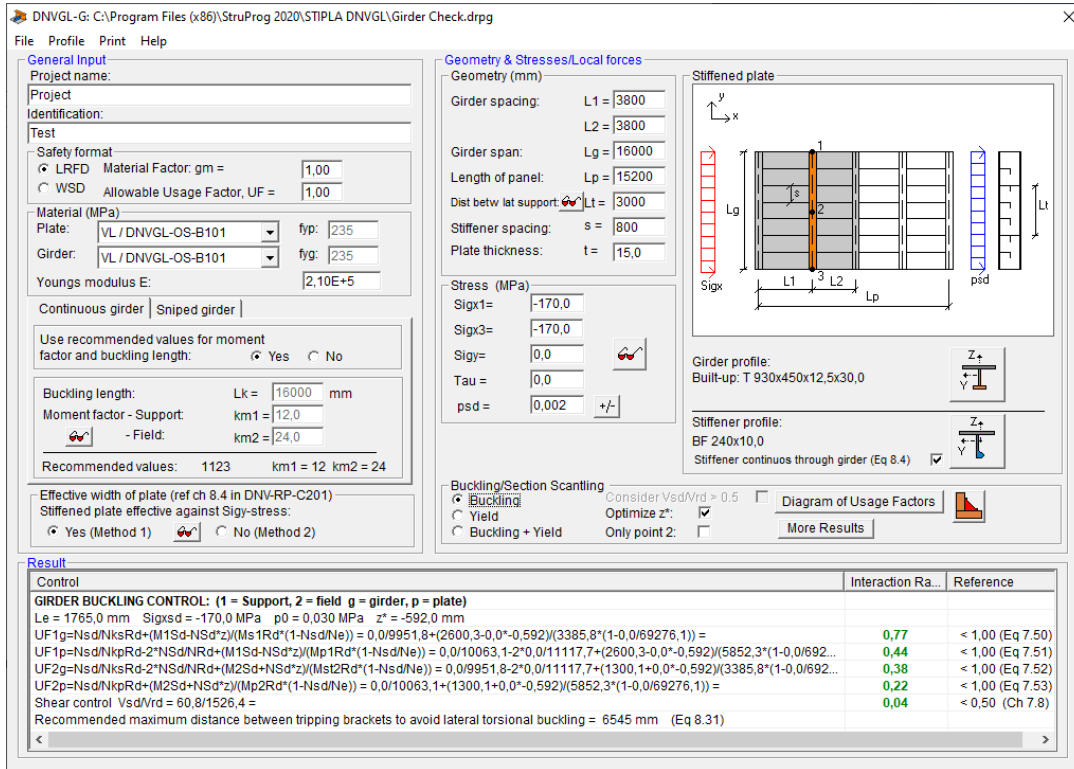


Figure 49 Girder Buckling check

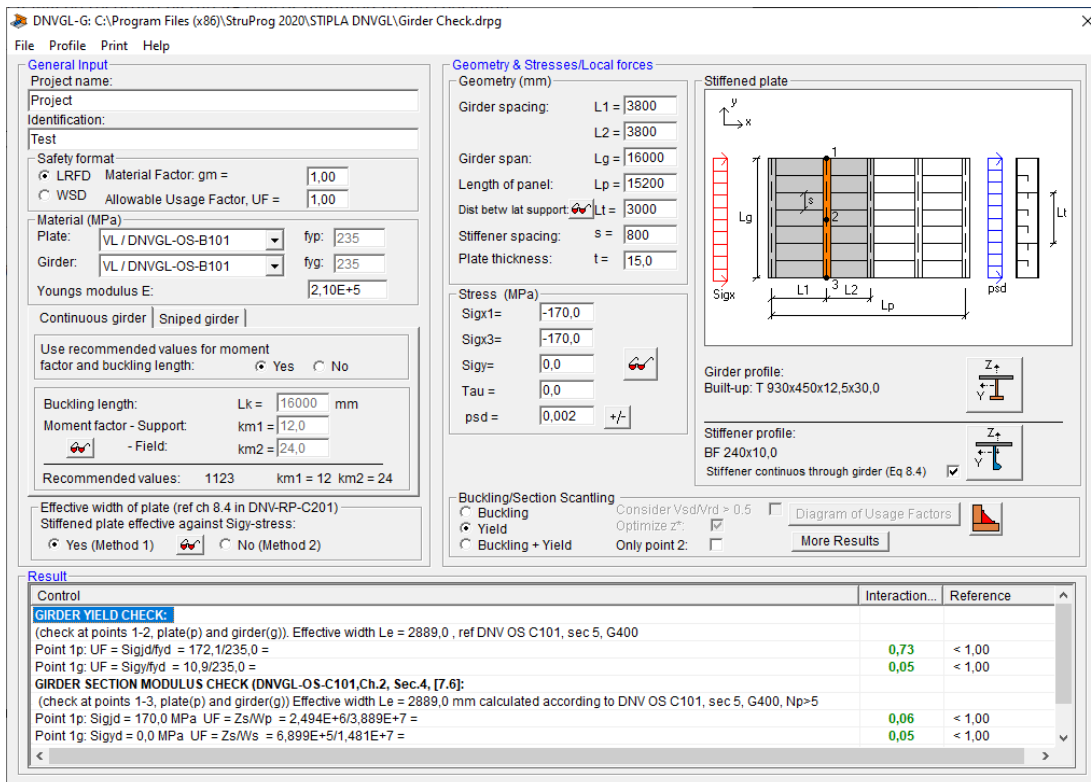


Figure 50- Girder yield check

DNVGL-G: C:\Program Files (x86)\StruProg 2020\STIPLA DNVGL\Girder Check.drp

File Profile Print Help

General Input

Project name:

Project Identification:

Test

Safety format
 LRFD Material Factor, gm = 1,00
 WSD Allowable Usage Factor, UF = 1,00

Material (MPa)
 Plate: VL / DNVGL-OS-B101 fyp: 235
 Girder: VL / DNVGL-OS-B101 fyg: 235
 Youngs modulus E: 2,10E+5

Continuous girder | Sniped girder |

Use recommended values for moment factor and buckling length: Yes No

Buckling length: Lk = 16000 mm
 Moment factor - Support: km1 = 12,0
 - Field: km2 = 24,0
 Recommended values: 1123 km1 = 12 km2 = 24

Effective width of plate (ref ch 8.4 in DNV-RP-C201)
 Stiffened plate effective against Sigy-stress:
 Yes (Method 1) No (Method 2)

Geometry & Stresses/Local forces

Geometry (mm)
 Girder spacing: L1 = 3800
 L2 = 3800
 Girder span: Lg = 16000
 Length of panel: Lp = 15200
 Dist betw lat support: Lt = 3000
 Stiffener spacing: s = 800
 Plate thickness: t = 15,0

Stress (MPa)
 Sigx1 = -170,0
 Sigx3 = -170,0
 Sigy = 0,0
 Tau = 0,0
 psd = 0,002 +/-

Buckling/Section Scantling
 Buckling Consider Vsd/Vrd > 0.5
 Yield Optimize z*:
 Buckling + Yield Only point 2:

Diagram of Usage Factors

More Results

Stiffened plate

Girder profile:
 Built-up: T 930x450x12,5x30,0

Stiffener profile:
 BF 240x10,0
 Stiffener continuous through girder (Eq 8.4)

Result

Control	Interaction...	Reference
GIRDER BUCKLING CONTROL: (1 = Support, 2 = field g = girder, p = plate)		
UF1g=Nsd/NksRd+(M1Sd-NSd*z)/(Ms1Rd*(1-Nsd/Ne)) = 0,0/9951,8+(2600,3-0,0*-0,592)/(3385,8*(1-0,0/69276,1)) =	0,77	< 1,00 (Eq 7.50)
Shear control Vsd/Vrd = 60,8/1526,4 =	0,04	< 0,50 (Ch 7.8)
GIRDER YIELD CHECK:(check at points 1-2, plate(p) and girder(g)). Effective width Le = 2889,0 , ref DNV OS C101, sec 5, G400		
Point 1p: UF = Sigjd/fyd = 172,1/235,0 =	0,73	< 1,00
GIRDER SECTION MODULUS CHECK (DNVGL-OS-C101, Ch.2, Sec.4, [7.6]): (check at points 1-3, plate(p) and girder(g))		
Point 1p: Sigjd = 170,0 MPa UF = Zs/Wp = 2,494E+6/3,889E+7 =	0,06	< 1,00
GIRDER WEB AREA: (DNVGL-OS-C101, Ch.2, Sec.4, [7.6]):		
Web area at support: twt = 0,57/12,5 =	0,05	< 1,00

Figure 51 Girder yield and buckling check